



Review

Critical Review of Temperature Prediction for Lithium-Ion Batteries in Electric Vehicles

Junting Bao ¹, Yuan Mao ^{1,*}, Youbing Zhang ¹, Hao Xu ¹, Yajie Jiang ² and Yun Yang ^{2,*}

¹ College of Information Engineering, Zhejiang University of Technology, Hangzhou 310014, China; 211122030107@zjut.edu.cn (J.B.); youbingzhang@zjut.edu.cn (Y.Z.); 221122030176@zjut.edu.cn (H.X.)

² School of Electrical and Electronic Engineering, Nanyang Technological University, Singapore 639798, Singapore; yajie.jiang@ntu.edu.sg

* Correspondence: maoyuan@zjut.edu.cn (Y.M.); yun.yang@ntu.edu.sg (Y.Y.); Tel.: +65-0571-85290582 (Y.M.)

Abstract: This paper reviews recent advancements in predicting the temperature of lithium-ion batteries in electric vehicles. As environmental and energy concerns grow, the development of new energy vehicles, particularly electric vehicles, has become a significant trend. Lithium-ion batteries, as the core component of electric vehicles, have their performance and safety significantly impacted by temperature. This paper begins by introducing the fundamental components and operating principles of lithium-ion batteries, followed by an analysis of how temperature affects battery performance and safety. Next, the methods for measuring and predicting battery temperature are categorized and discussed, including model-based methods, data-driven methods, and hybrid approaches that combine both. Finally, the paper summarizes the application of temperature prediction in a BMS and provides an outlook on future research directions.

Keywords: lithium-ion battery; thermal management; temperature prediction; thermal runaway; electrochemical model; data-driven method



Citation: Bao, J.; Mao, Y.; Zhang, Y.; Xu, H.; Jiang, Y.; Yang, Y. Critical Review of Temperature Prediction for Lithium-Ion Batteries in Electric Vehicles. *Batteries* **2024**, *10*, 421. <https://doi.org/10.3390/batteries10120421>

Academic Editors: Abbas Fotouhi and Elham Hosseinzadeh

Received: 11 November 2024

Revised: 25 November 2024

Accepted: 26 November 2024

Published: 29 November 2024



Copyright: © 2024 by the authors. Licensee MDPI, Basel, Switzerland. This article is an open access article distributed under the terms and conditions of the Creative Commons Attribution (CC BY) license (<https://creativecommons.org/licenses/by/4.0/>).

1. Introduction

In recent years, due to the worsening climate and environmental conditions and the gradual decline in the production of various energy materials, the energy industry has been continuously transitioning and upgrading in search of more environmentally friendly and cleaner energy sources [1,2]. In this era of new energy development, traditional fuel-powered vehicles, due to their harmful emissions and reliance on diesel, are being increasingly replaced by new energy vehicles, a trend driven by the current low-carbon economy [3,4]. Among these, all-electric vehicles stand out as the most popular representatives of new energy vehicles, offering higher energy efficiency and nearly zero emissions compared to traditional fuel-powered cars [5,6]. Lithium-ion batteries are widely used as power sources in electric vehicles due to their advantages of high voltage, high current, high energy density, low self-discharge rate, light weight, long cycle life, and environmental friendliness [6,7]. The structure of a lithium-ion battery typically consists of a cathode, electrolyte, and anode. Generally, lithium-ion composite materials, such as lithium iron phosphate, lithium manganese oxide, and lithium cobalt oxide, are used as cathodes, while graphite is predominantly used as the anode [8,9].

However, under normal conditions, lithium iron phosphate batteries typically operate within a temperature range of 0–60 °C, while ternary lithium batteries can function at temperatures as low as –20 °C [10]. Additionally, research [11] suggests that the acceptable operating temperature range for lithium-ion batteries is approximately –20 to 60 °C, while [12] identifies 20–40 °C as the optimal range for their operation. If the temperature exceeds this range, excessive chemical reactions may occur within the battery, negatively impacting its cycle life, performance, safety, and reliability [13–15]. Extremely high temperatures may even lead to thermal runaway and potential explosions [16,17]. Therefore,

to ensure safe operation within a reasonable temperature range, a BMS is essential. It provides real-time and precise monitoring of various parameters, such as voltage, current, and temperature [18], and uses these data to estimate the battery's SOC, SOH, RUL, SOP, and SOT [19]. Additionally, parameters like internal resistance [20], remaining capacity [21], SOC [22], and SOH [23] are all influenced by temperature, making accurate temperature prediction crucial for precise estimation of the battery's condition. The BMS also ensures the balance of the battery pack and provides real-time fault monitoring and diagnosis. This guarantees efficient operation, safety, and extended battery life, all of which require detailed temperature information for individual cells and the entire battery pack [24–26]. Accurate temperature data from both the core and surface of the battery are critical for effective thermal management and safety, as the temperature difference between the core and surface can reach up to 10 °C during operation [27].

Currently, there are two main methods for obtaining battery temperature: measurement and estimation [28,29]. Measurement methods can be further divided into contact and non-contact methods [30]. Contact measurement primarily uses various sensors, such as thermistors and thermocouples, to collect data. These sensors are typically embedded directly inside the battery, enabling rapid and accurate detection of internal temperature changes for real-time monitoring and thermal runaway warnings [31]. However, this method presents challenges in practical use, such as the high precision required of the sensors and the risk of compromising the battery's seal, which could lead to leakage and affect performance [32,33]. Additionally, internal sensors may react with battery materials, leading to corrosion. Over time, this could shorten the sensors' lifespan and result in data inaccuracies [34]. Non-contact methods include battery modeling and electrochemical impedance techniques. Battery modeling involves creating models based on certain physical or chemical properties to simulate temperature changes [35]. Electrochemical impedance mapping relates battery resistance to temperature to track thermal variations [36]. These non-contact methods typically require specific physical or chemical parameters, but the various operating conditions during actual use make real-time monitoring difficult, leading to inaccuracies in temperature representation. As a result, many studies now use various algorithms to estimate battery temperature. These estimation methods can be broadly categorized into model-based approaches [37–39], data-driven methods [40–42], and hybrid approaches combining both model and data-driven methods [43]. These methods model parameter variations during battery operation to predict temperature by establishing explicit or implicit relationships between temperature and other parameters.

This paper presents the heat generation principles of lithium-ion batteries during operation and the changes in battery mechanisms during thermal runaway. It also summarizes the impact of temperature fluctuations on battery lifespan and safety. The paper categorizes the methods for predicting lithium-ion battery temperature and analyzes the issues associated with current prediction techniques. By discussing various prediction methods, this paper provides a possibility for improving the accuracy of the temperature prediction module in a future BMS. At the same time, a high-precision BMS, in turn, improves the safety and reliability of the battery, providing solutions to safety challenges in extreme environments and different operating conditions.

2. Theory of Heat Generation and Thermal Runaway of Lithium-Ion Battery

Efficient battery monitoring and control are essential for ensuring high performance, longevity, and safety during battery operation. During operation, lithium-ion batteries inevitably undergo internal chemical reactions. These reactions, along with the associated loss of battery material and internal resistance, generate heat, causing the internal temperature of the battery to rise [44]. As the battery's temperature increases, its internal resistance decreases, accelerating aging and capacity loss, which shortens the battery's lifespan. Excessive heat can even lead to overheating, thermal runaway, or severe incidents like explosions [45]. Therefore, to ensure safe operation, it is crucial to monitor the battery's temperature effectively and with high precision [46]. The foundation of temperature mon-

itoring lies in understanding the basic principles of heat generation in batteries and the impact of temperature fluctuations on battery performance. Additionally, understanding the mechanisms and principles of thermal runaway is necessary to provide early warnings and implement control measures [47].

2.1. The Principle of Battery Heat Generation

Lithium-ion batteries continuously release and absorb heat during charging and discharging cycles [48]. According to basic thermodynamic principles, the battery maintains this condition under constant temperature. Thus, the heat released during the reaction, denoted as ΔG [49], can be equated to Gibbs free energy in thermodynamics, as shown in Equation (1):

$$\Delta G = \Delta H - T\Delta S \quad (1)$$

Here, ΔH represents the change in enthalpy within the battery. T is the absolute temperature, which can be obtained from the sensor, and ΔS is the change in entropy. Thus, if the charging and discharging processes are defined as reverse reactions, the absorption and release of heat by the battery will also be reverse processes. In Equation (1), $T\Delta S$ represents the thermal energy of the reaction during battery operation. Therefore, the heat generated by the battery reaction, Q_r , is defined as:

$$Q_r = T\Delta S = -T \frac{\delta \Delta G}{\delta T} \quad (2)$$

If the EMF of the battery is E_e , it can be obtained through HPPC experiments or simulated through models. The Faraday constant is F , and the number of charges involved in the reaction is n , and Equation (2) can be rewritten as:

$$\begin{cases} \Delta G = -nFE_e \\ Q_r = nFT \frac{\delta E_e}{\delta T} \end{cases} \quad (3)$$

During the charging and discharging process of a battery, the reaction heat Q_r is related to the embedding and de-embedding of lithium ions. During charging, the process is heat-absorbing when lithium ions are dislodged from the positive electrode material, while during discharging, the process is exothermic when lithium ions are embedded in the negative electrode material. This reversible heat is related to the open-circuit voltage of the battery's state of charge and is similarly related to the SOC, with the sign and magnitude of the reversible heat changing at different SOC.

In practice, during the charging and discharging processes, lithium-ion batteries also experience polarization resistance in addition to reaction heat Q_r . This polarization, caused by ohmic polarization, concentration polarization, and electrochemical polarization, results in a voltage drop and generates additional heat [50]. The heat lost due to polarization is defined as polarization heat Q_p . Additionally, during internal reactions, there are side reactions and self-discharge phenomena [51]. The heat generated from these side reactions is defined as side reaction heat Q_s . Among them are side reactions, such as electrolyte decomposition and SEI film formation and growth, which are usually heat-absorbing. The heat produced from Joule heating due to the battery's resistance is defined as Joule heat Q_j . This heat is generated as an exothermic reaction during both charging and discharging processes. The total heat generated by the battery during reactions, Q_t , is defined as follows [52]:

$$Q_t = Q_r + Q_p + Q_s + Q_j \quad (4)$$

However, during the battery charging and discharging processes, the impact of side reaction heat Q_s is minimal and is more related to the aging process of the battery. Therefore, Q_s can be neglected in Equation (4). In contrast, the heat generated due to increased battery resistance, Q_j , has a significant impact on the battery temperature compared to self-discharge processes. Therefore, it cannot be ignored. Similarly, polarization heat Q_p

generated during battery operation cannot be overlooked. Therefore, the heat generated by the battery during operation, as given in Equation (4), can be simplified to:

$$Q_t = Q_r + Q_p + Q_j = nFT \frac{\delta E_e}{\delta T} + Q_p + Q_j \quad (5)$$

In current battery heat generation models [53], polarization heat Q_p and Joule heat Q_j are defined based on heat generation principles. Joule heat Q_j is the heat generated by battery current through a resistor during battery operation, and its calculation is defined by Joule's law as follows:

$$Q_j = I^2 R_e \quad (6)$$

In the equation, I represents the current variation during the battery charging and discharging processes, which is acquired through real-time sensor acquisition during the experiment. R_e denotes the battery's ohmic resistance, which is usually obtained by model identification. It is affected by factors including the external environment and the inherent properties of materials. Similarly, while polarization is due to the presence of polarization resistance within the cell, it is essentially due to different internal resistances generating heat. Its calculation formula is as follows:

$$Q_p = I^2 R_p = I^2 (R_o + R_n + R_d) \quad (7)$$

Here, R_p represents the battery's polarization resistance; R_o denotes ohmic polarization resistance; R_n stands for concentration gradient resistance; and R_d refers to electrochemical polarization resistance. Therefore, Ref. [54] extends the battery heat generation model from Equation (5) as follows:

$$Q_t = I(IR_e + IR_p) + IT \frac{\delta E_e}{\delta T} = I \left[(E_e - E) + T \frac{\delta E_e}{\delta T} \right] \quad (8)$$

where E represents the end voltage value of the battery in the process of charging and discharging, which is obtained in a similar way to I and is obtained through sensor acquisition.

The above describes the heat generated by the battery during normal operation. Under typical conditions, reaction heat, Joule heat, and polarization heat are the primary components of battery heat. However, in extreme situations, such as thermal runaway, the heat composition of the battery becomes more complex. In such cases, internal chemical reactions may occur, and conditions like overcharging and over-discharging can introduce additional heat sources. Furthermore, external scenarios involving thermal abuse can also affect the battery's heat composition [55].

2.2. Thermal Runaway Principle of Battery

In practical use, the operating conditions and environment of lithium-ion batteries are often unknown. This means that batteries may operate in extreme environments or under conditions that could cause damage. Various conditions inevitably affect the performance and safety of lithium-ion batteries. Severe misuse can lead to thermal runaway and even explosions [56]. Misuse of lithium-ion batteries can be categorized into thermal abuse, electrical abuse, and mechanical abuse [57]. During thermal runaway, there may be interactions and influences from various types of abuse. Regardless of the type of abuse, it ultimately leads to internal short-circuiting and thermal runaway [58].

Among all the causes of thermal runaway, thermal abuse seems to be the most direct. This includes excessively high ambient temperatures or overheating of certain parts of the battery. Such elevated temperatures cause various reactions within the battery, further increasing its temperature and leading to thermal runaway [59]. As previously analyzed, at normal operating temperatures (0–50 °C), the heat generated by the battery primarily includes reaction heat, Joule heat, and polarization heat. As the battery temperature continues to rise, the SEI layer on the negative electrode begins to decompose, leading to further reactions between the negative electrode and the electrolyte. This results in

the decomposition of the electrolyte and initiates self-heating of the battery [60]. After self-heating, the battery's internal separator begins to shrink. As the temperature continues to rise, the separator can break down, leading to internal short-circuiting [61]. This thermal short circuit accelerates internal reactions, and the positive electrode starts reacting with the electrolyte, leading to thermal runaway in the battery.

Similar to thermal abuse, electrical abuse is also a common issue during battery operation. This includes phenomena such as external short-circuits and overcharging or over-discharging of the battery [62–64]. External short-circuiting of the battery causes a rapid increase in current, which results in significant Joule heating and gas release from the battery. Prolonged short-circuiting can lead to dangerous conditions, such as swelling, leakage, or rupture of the battery. Overcharging is much more dangerous than external short-circuiting. When the battery is overcharged beyond its nominal capacity, the negative electrode becomes saturated with lithium, preventing lithium ions from attaching to it. This leads to the formation of metallic lithium on the negative electrode surface, reducing the number of lithium ions and exacerbating polarization reactions [65]. The formation of metallic lithium can lead to lithium crystallization on the electrode surface, which damages the separator and causes internal short-circuiting, ultimately leading to thermal runaway. Additionally, the lithium layer reacts further with the electrolyte, causing continuous temperature rise and gas release inside the battery, which can lead to swelling, rupture, and thermal runaway [64]. In contrast to overcharging, over-discharging occurs when the battery capacity is too low. This can lead to fluid dissolution at the negative electrode, causing copper deposition similar to lithium deposition, which may puncture the separator and result in internal short-circuiting.

Mechanical abuse involves external forces on the battery, such as punctures, compression, or collisions. These forces can damage the battery separator, leading to internal short-circuiting and rapid heat release, which can cause thermal runaway [66]. In addition to separator damage, a broken battery casing allows air to enter the battery, react with the electrolyte, and produce significant amounts of heat [67]. These conditions often lead to further instances of thermal abuse. In some cases, mechanical forces may cause deformation of the battery body without causing a rupture. This deformation can lead to localized electrode strain or separator damage, resulting in internal short-circuiting and potentially triggering thermal runaway.

According to the above analysis of the three failure forms of different forms of abuse, it can be found that these three kinds of abuse are often not independent of each other; usually, the occurrence of a form of abuse leads to the rest of the abuse of the chain reaction and finally to the overheating of the battery. In fact, the different abuse of battery damage is caused in different locations, with the impact of mechanical abuse and electrical abuse of the intrinsic factors, including the diaphragm, electrolyte, and casing, and the thermal runaway characteristics of the temperature of the determining factors mainly for the battery's internal materials, such as electrodes, electrolytes, and the thermal stability of the diaphragm. Figure 1 shows the internal and external reactions of a battery under different abuse conditions.

After a battery is subjected to different abusive effects that lead to increasing battery temperature, the electrochemical reactions within the battery during thermal runaway can be mainly divided into the following reactions: in the early stage of thermal runaway, the SEI film on the surface of the negative electrode of the battery starts to decompose, which is an exothermic reaction, and the heat generated leads to a further increase in the temperature of the battery [68]. As the temperature rises further, the side reaction between the electrolyte and the negative electrode material intensifies, and gases such as CO and CO₂ are released. When the internal temperature of the battery reaches the melting point of the diaphragm material, the diaphragm starts to melt, which leads to direct contact between the positive and negative electrodes inside the battery, triggering a serious internal short circuit, thus generating a large amount of heat. At high temperatures, the positive electrode material may decompose, releasing oxygen. The electrolyte will also decompose

at high temperatures, generating heat and gases. These gases include flammable gases such as hydrogen and hydrocarbon gases, which may react with the oxygen inside the battery to trigger combustion [69]. The binder in the battery electrodes may also decompose at high temperatures, generating additional heat and gases. In the later stages of thermal runaway, the electrolyte may react violently with the oxygen released from the positive electrode, leading to electrolyte combustion, which is the most violent exothermic reaction in the thermal runaway process.

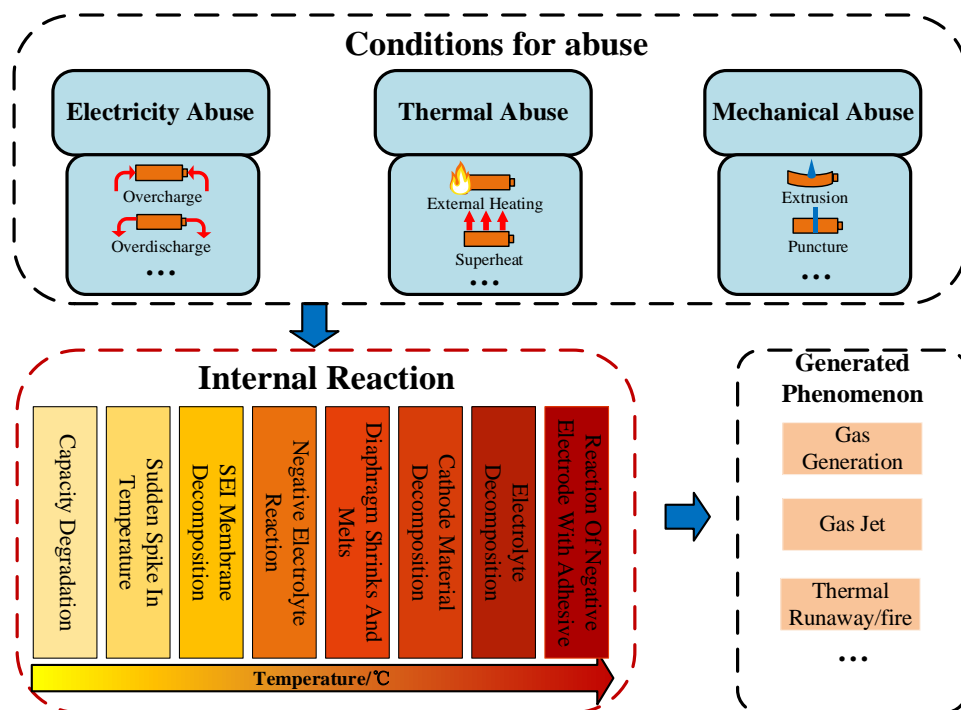


Figure 1. Internal and external thermal runaway of battery under different abuse conditions.

The entire thermal runaway process is a chain reaction that is difficult to control once it starts. The temperature inside the battery rises dramatically, leading to the destruction of the battery structure, which may cause the battery to catch fire or even explode. Therefore, the design of the thermal management system of the battery is crucial to prevent the occurrence of thermal runaway.

2.3. The Influence Mechanism of Temperature on the Battery

Environmental temperature has a significant impact on battery performance and safety. Within the normal operating temperature range, the heat generation of the battery is described by Equation (8), and under normal conditions, thermal runaway does not occur. It is important to note that during high-rate charging or discharging, the battery's internal resistance increases rapidly, causing the temperature to rise continuously. This can lead to thermal abuse, which needs to be managed. M. Keyser et al. [70] simulated high-rate charging of an 18 Ah NCM pouch battery at 350 kW under poor cooling conditions, finding that the battery temperature could reach 350 °C within 750 s, a temperature at which thermal runaway can begin. Additionally, during idle periods, the self-discharge rate and internal resistance of a battery are affected by environmental temperature. Therefore, it is essential to account for the battery's sensitivity to temperature to maximize energy utilization while ensuring safety [71]. Lithium-ion batteries can be exposed to extreme temperatures, with low temperatures defined as below 0 °C and high temperatures as above 50 °C.

When the battery is in low-temperature conditions, different low-temperature zones have different impacts on the performance and safety of lithium-ion batteries. At 0 to –10 °C,

the battery can still operate normally, but at this time, the lithium-ion diffusion coefficient of the anode material decreases, and the charge transfer impedance increases; the lithium-ion intercalation reaction of the anode material slows down, and the charging and discharging efficiency of the battery decreases, which affects the acceleration performance of the electric vehicle. At $-10\text{ }^{\circ}\text{C}$ to $-20\text{ }^{\circ}\text{C}$, the positive electrode material may have structural changes, such as transition metal migration or phase transition. Lithium-ion deposition begins to occur on the surface of the negative electrode material, forming lithium metal deposits and increasing the risk of short circuits within the battery. The fluidity of the electrolyte decreases, which may lead to poor contact between the electrolyte and the electrodes, at which time the charging capacity of the battery is already limited, and in order to ensure the safety of the battery, it is necessary to use a smaller charging current and increase the charging time [72]. The diffusion of lithium ions from the positive electrode material slows down significantly from $-20\text{ }^{\circ}\text{C}$ to $-30\text{ }^{\circ}\text{C}$, which may lead to structural damage in some materials. Lithium deposition in the anode material becomes more severe, and lithium dendrites may form, posing a threat to the safety of the battery. The electrolyte may begin to solidify, seriously affecting the charging and discharging capacity of the battery. At this time, the battery discharge capacity may drop by 30% to 50% of the room temperature capacity, and below $-30\text{ }^{\circ}\text{C}$, the battery's discharge capacity at this time is so low that it can no longer work normally, and the performance of the positive electrode material decreases dramatically, and structural damage may occur, affecting the long-term stability and cycle life of the battery [73]. The growth of lithium dendrites in the negative electrode material may lead to the destruction of the internal structure of the battery. Most of the components of the electrolyte may have solidified, and lithium-ion transport inside the battery will have almost stopped. In general, when the battery is in a low-temperature environment, according to Arrhenius Equation (9), the activation energy E_a for reactions increases. This reduces charge transfer kinetics and electrochemical characteristics and decreases the ion diffusion rate K in the electrolyte, leading to increased battery polarization. However, some studies have been conducted to address the performance and safety hazards of lithium-ion batteries at low temperatures by adopting potassium ions as a substitute [74] or substituting electrolyte materials [75] to achieve capacity retention at low temperatures. At this point, the rate of lithium deposition on the negative electrode greatly exceeds the rate of lithium intercalation, reducing the number of lithium ions in the battery and decreasing its usable capacity. Excessive lithium deposition can form lithium dendrites, which may puncture the separator and pose a risk of electrical abuse [76].

$$K = Ae^{-\frac{E_a}{RT}} \quad (9)$$

At high temperatures, such as $50\text{ }^{\circ}\text{C}$, the battery surface temperature and voltage differences begin to intensify, indicating that high temperatures begin to affect the overall temperature uniformity of the battery. The increase in heat generation of the battery leads to an increase in the surface temperature of the battery, especially during the discharge process. The battery capacity decay rate increases, and the high temperature accelerates the battery aging process; as the temperature rises further to $60\text{ }^{\circ}\text{C}$, the thermogenesis and internal chemical reaction of the battery become more intense, and the battery performance begins to decline significantly. The inconsistency of the battery is further aggravated, and the temperature and voltage differences increase, which increases the complexity of battery pack management. The battery capacity decay rate further increases, and the battery life is shortened [77]; after the battery temperature reaches $70\text{ }^{\circ}\text{C}$ or even higher, the thermogenesis of the battery reaches its maximum, at which time the battery performance is seriously affected, and the overall temperature variability of the battery is so great that the battery may undergo thermal runaway phenomenon if cooling treatment is not performed. Compared with the low-temperature environment, the high-temperature environment brings more obvious damage to Li-ion batteries. From the material point of view, the high temperature stimulates the growth of SEI and the degradation of cathode materials inside Li-ion batteries, which increases the polarization effect of the batteries [78]. At the same time, the degradation of cathode materials while generating gases accelerates the degradation of battery capacity;

in addition, high temperatures may exacerbate the inhomogeneity inside the battery, leading to localized overheating and increasing the risk of thermal runaway and combustion [79]. Therefore, high temperature is an environmental factor that requires special attention during the use and storage of lithium-ion batteries. Therefore, thermal management systems for batteries are particularly important under high-temperature conditions. Some studies exist that use PCM as an effective thermal management strategy [80]. PCM absorbs heat when the battery temperature increases and releases heat when the temperature decreases, which helps to maintain the stability of the battery temperature. It has been shown that the thickness of PCM has a significant effect on the stability of battery temperature change, discharge performance, and capacity decay rate.

To ensure battery performance and safety, it is necessary to control the environmental temperature during operation or use a BTMS to regulate the battery temperature. This helps maintain the operating temperature within a safe range while maximizing energy utilization [81].

2.4. Impact of Battery Packs on Battery Temperature Variations

In addition to the temperature variation of a single cell, in practical applications, batteries are often used as energy storage elements in battery packs consisting of multiple cells. The battery pack use process is accompanied by a large amount of charging and discharging, resulting in the expansion of the temperature difference between battery packs. In addition, the battery pack of individual cells due to the internal resistance of the battery is different or the cooling intensity of the difference between the temperature of the single cells within the group will inevitably appear. The different arrangement of the battery pack will also cause the battery pack monomer as the other monomers are influenced by different sizes. Therefore, in order to give full play to the role of the battery pack as an energy storage device and guarantee the life and safety of the battery pack, the battery pack management system should formulate appropriate thermal management and energy management strategies according to the thermal behavior of the battery pack.

The thermal behavior of lithium-ion battery packs is related to factors such as the structure of the battery pack, environmental temperature, and cooling strategy, among other factors. Therefore, it is important to establish a heat transfer model that accurately describes the thermal behavior of battery packs for the development of a temperature management system for battery packs. The three-dimensional thermal model of a square lithium-ion battery pack was established in ref. [82], and the model can be used to improve the structural details of the battery pack and thermal management system, but its calculation is complicated and not applicable to the onboard battery pack management system. A one-dimensional transient heat transfer model for a square lithium-ion battery pack was developed in the literature [83]. The model considers the effects of the battery pack's ambient temperature, initial SOC, operating load, and cooling intensity on the operating temperature of each individual cell in the battery pack. The authors of ref. [84] proposed the definition of energy and power utilization and quantitatively analyzed the effect of temperature inconsistency on the discharge performance of series-connected battery packs based on a second-order RC model.

In addition to modeling the battery pack to capture the temperature variability in the battery pack under different conditions, it is also necessary to consider the effect of temperature spreading effects within the battery pack under thermal runaway conditions on the safety of the battery pack. As the number of cells in a battery pack increases, thermal conduction between cells causes heat to be transferred within the pack. This thermal conduction increases the thermal resistance of the battery pack, making it difficult for heat to build up inside individual cells, thus increasing the amount of heat flow required to trigger thermal runaway [85]. The closer the cells in a battery pack are to an external heat source, the earlier the thermal runaway is triggered and the higher the onset temperature. This means that the resistance of cells near an external heat source may decrease as the temperature rises, while cells farther away from the heat source require higher temperatures

to achieve the same resistance change [86]. Based on the thermal runaway of battery packs, ref. [87] conducted cooling tests based on the thermal runaway battery pack model and found that aerogel can effectively cut off the direct heat transfer from different cells, preventing the ignition of the surrounding cells when the heat of the cell is out of control; the mica plate can disperse the heat emitted by the battery, preventing the heat from accumulating at a certain point and leading to burn-through of the battery shell. Different microchannel widths and coolant flow rates for cold plates in LIB batteries were used to check the effectiveness of thermal runaway suppression. The numerical model was validated by experimental measurements, and the heat loss of the coolant and its ratio to the total heat released were quantitatively examined. Critical curves to distinguish between thermal runaway and non-thermal runaway scenarios were determined to characterize the key conditions for thermal runaway suppression [88]. Therefore, the temperature change of the battery pack is more complicated and affected by more factors than the battery cells. At the same time, the control of the temperature spread between the battery cells in the battery pack is the key to ensuring the consistent temperature of the battery, inhibiting the thermal runaway of the battery, and ensuring normal operation of the battery pack.

3. Simple Framework for Temperature Analysis of Lithium-Ion Battery

Based on the research into temperature effects on batteries, it is observed that heat is generated during both charging and discharging, regardless of the battery's chemical properties. Some of this heat is dissipated through the battery materials, while the rest accumulates inside the battery. If the rate of heat dissipation is much lower than the internal heat generation rate, it may lead to excessively high temperatures at the battery surface and core, with a risk of thermal runaway. This issue becomes more pronounced in extreme conditions and operational scenarios. Therefore, conventional temperature prediction models typically use certain chemical or physical properties of the battery to establish corresponding thermal generation and heat transfer models [53] for temperature estimation. Some adaptive studies also consider various battery states, such as SOC and SOH, and develop related functions to estimate temperature through models. Additionally, some studies use data-driven approaches to avoid disturbances in property calculations by employing black-box self-learning techniques to uncover hidden relationships between battery parameters and temperature changes, thus creating highly accurate temperature prediction models. Nonetheless, fundamental similarities exist among lithium-ion battery temperature prediction models, and a general temperature estimation strategy model is illustrated in Figure 2.

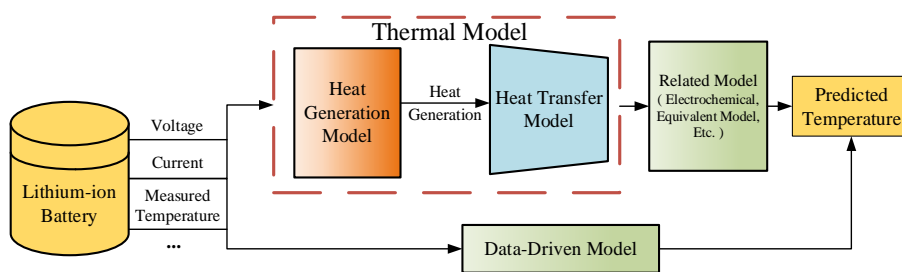


Figure 2. Common lithium-ion battery temperature prediction frame diagram.

4. Lithium-Ion Battery Temperature Prediction Method

As discussed in the previous section, the goal of temperature prediction methods is to obtain highly accurate heat generation and heat transfer models. Heat generation models, in particular, can generally be classified into model-based and data-driven approaches. Model-based methods can further be divided into electrochemical models, equivalent circuit models, and black-box models, depending on the theoretical basis for heat generation. Additionally, based on the definition of heat sources within the battery, these models can be categorized into lumped [89], distributed [90], and heterogeneous [91] heat generation models. The lumped heat generation model is relatively simple and treats the battery as a

single heat source. It does not require detailed knowledge of the battery's materials, internal structure, or specific parameters—just the current–voltage curve—to fit the necessary parameters. In contrast, the distributed heat generation model views the entire battery as a uniform heat source, while the heterogeneous model differentiates heat generation across various layers within the battery, typically resulting in a temperature gradient from the interior to the surface. Unlike heat generation models, heat transfer models must consider the impact of different battery materials on heat conduction. Common heat transfer models include FEA and thermal capacity–thermal resistance models [92]. The FEA model is an idealized approach that typically disregards environmental interactions and divides the battery into finite elements for heat transfer calculations [93]. The thermal capacity–thermal resistance model, on the other hand, equates circuit parameters with those of a thermal system to represent heat transfer [94]. However, thermal capacity–thermal resistance models have limitations in representing heat transfer, as they generally only reflect temperature changes within a single dimension, whereas a battery's temperature distribution is not uniform across all directions. Furthermore, the computational load required for online prediction is significantly increased by the nonlinear calculations necessary to represent complete battery heat transfer using complex thermal capacity–thermal resistance models.

Therefore, a complete system that uses heat generation outputs from the heat generation model as inputs to the heat transfer model is referred to as a thermal model. This thermal model estimates the temperature changes in a battery during operation. In common model-based battery temperature estimation, methods can be categorized based on the type of model used, such as electrochemical models, EECM, and direct impedance measurement [95]. In addition, data-driven methods and hybrid approaches combining data-driven methods with models attempt to bypass the complexities of model development. They achieve this using neural networks to map the hidden relationships between battery temperature and other parameters, thus predicting battery temperature. This section will, therefore, discuss and compare different temperature prediction methods.

4.1. Model-Based Prediction

A significant portion of current research on battery temperature prediction relies on modeling methods, with many simulation techniques based on physical principles already developed. For example, the Newman model can simulate the thermal field distribution within a battery, while the Bernard model can analyze heat generation. However, these physical models have several limitations. First, batteries vary in material, size, composition, and packaging depending on the type and manufacturer. Additionally, the complex and diverse usage environments and load conditions make these methods challenging to apply at scale for real-time online estimation.

4.1.1. Based on Electrochemical Model

The electrochemical–thermal coupling model assumes a uniform current distribution within the battery, integrating the heat generated from internal chemical reactions to describe the battery's heat generation mechanism. Therefore, before constructing such a model, it is essential to obtain information on ion concentration and migration speed in both the solid and liquid phases near the lithium-ion battery's current collectors. This model is more suitable for small batteries due to its assumption of uniform current density. For larger batteries, significant errors may occur during simulation. Most temperature prediction studies based on electrochemical models can be categorized into one-dimensional models that focus on one direction within the battery, two-dimensional models that analyze reactions within a specific plane, and three-dimensional models that consider the entire battery.

The one-dimensional (1D) model is the simplest battery model, assuming that all physical and chemical processes inside the battery occur in a single direction, typically along the thickness of the electrode. This model is commonly used in lithium-ion batteries where the electrode thickness is much greater than its width and length. The 1D model effectively captures concentration gradients and potential distributions within the electrode

but overlooks the complexities at the electrode surface. For instance, ref. [27] used a radial 1D model combined with EIS and surface temperature measurements to estimate the non-uniform internal temperature distribution of lithium-ion batteries in real time. This method does not require knowledge of the battery's thermal properties, heat generation, or thermal boundary conditions. Instead, it estimates temperature distribution by measuring the real or imaginary part of the battery impedance at a single frequency along with surface temperature. The authors of ref. [96] developed a single-particle model based on the principle of energy conservation to analyze the heat generated during different polarization processes in lithium-ion batteries, including polarization heat, ohmic heat, and reaction heat. The temperature simulation results using this single-particle model are shown in Figure 3. In ref. [97], the authors created an extended SP thermal coupling model that incorporates the temperature dependence of parameters such as solid-phase diffusion coefficients, electrochemical reaction rate constants, and OCPs of both electrodes. In the thermal coupling portion, parameters like solid-phase diffusion coefficients and electrochemical reaction rates are updated in real time to approximate the solution of the concentration polarization process. Ref. [98] developed a thermal analysis model for prismatic and rectangular battery packs based on battery cell test results. This model considers heat transfer within internal air layers and simplifies the representation to focus solely on conduction heat transfer. The simplified thermal analysis model confirmed that the internal temperature distribution of battery packs varies with shape, emphasizing the importance of considering battery pack shape in thermal management design. The authors of ref. [99] developed a radial 1D model and proposed a model-based approach that uses polynomial approximation to estimate the internal temperature distribution of the battery. This approach applies the DKF to identify convection coefficients and estimate the core temperature of cylindrical batteries. It accurately predicts core temperature under unknown convection cooling conditions by measuring battery current, voltage, surface temperature, and ambient temperature. In ref. [100], the authors used a 1D model to simulate the temperature field of lithium-ion batteries during charge and discharge processes, with a focus on the role of phase change materials in battery thermal management. The study analyzed the effects of different operating conditions and cooling rates on the thermal distribution within the lithium-ion battery. The authors of ref. [101] used a method of inserting thermocouples into the battery to measure internal temperature variations. The study found that during operation, the temperature difference between the internal and external parts of the battery could reach up to 10 °C. Using the measured parameters, a 1D model was developed, with simulation results differing from the experimental data by less than 1.5 °C. This method demonstrates good feasibility and offers valuable insights, given the challenges of measuring internal battery temperatures.

The two-dimensional (2D) model typically accounts for the physical and chemical processes occurring in two directions inside the battery, often along the width and length of the electrodes. This model is suitable for batteries with electrodes that have complex geometries or surface characteristics, such as certain types of supercapacitors or fuel cells. Based on the two-dimensional model, ref. [102] investigated the generation and evolution law of irreversible heat inside the lithium-ion battery, and the results showed that the irreversible heat increases rapidly with the increase in the discharge rate, and the size of the anode active particles has an important effect on the irreversible heat and polarization heat of the battery. The authors of ref. [103], based on this model, investigated the temperature condition of the battery lugs under a high-rate discharge and found that the lug temperature is an important reason for the equalization of the battery, and the lug size was optimized to improve the temperature distribution uniformity of the battery. In ref. [104], the authors investigated the inhomogeneity of temperature difference in large lithium batteries, and the results showed that the maximum temperature difference of large lithium batteries could reach 8.3 °C at a 2 C discharge rate. The authors of ref. [105] developed a coupling method between a 1D electrochemical submodel and a 2D thermoelectronic model. They used the 1D electrochemical submodel to calculate the heat production rate of the lithium-

ion battery, while the 2D thermoelectronic model was used to resolve the temperature on the surface of the lithium-ion battery, which effectively simulated the voltage and the heating rate of the lithium-ion battery. Its temperature distribution on the 2D model is shown in Figure 4. In ref. [106], the authors developed an electrochemical–thermal coupling model for polymer lithium-ion batteries, simulated the temperature distribution and heat generation rate of the batteries under different discharge currents, and obtained the temperature changes in different states. The authors of ref. [107] developed a time-domain method to determine the internal temperature of a battery from pulse resistance, which does not require additional excitation hardware to generate specific sinusoidal signals or complex filters and conversions to extract the spectrum from current and voltage time–domain measurements of a battery management system. In ref. [108], the authors developed a two-dimensional transient heat transfer model for simulating the temperature distribution of lithium-ion batteries under different heat dissipation methods and found that the temperature rise of the battery accelerates and the temperature difference between the inside and outside of the battery increases with the increase in battery SOC and discharge current. The use of forced convection can reduce the surface temperature of the battery, but it increases the temperature distribution inhomogeneity of the battery. The authors of ref. [109] provided a two-dimensional thermal model for cylindrical Ni/MH batteries to analyze the thermal behavior of the batteries during charging and overcharging, and the heat and heat generation rates of the batteries during charging and overcharging were investigated by a quartz-frequency microcalorimeter, and the heat generation curves were fitted. In addition to the two-dimensional model, the P2D chemical model, as a kind of multiscale model between one-dimensional and three-dimensional models, was proposed in 1993, which made some assumptions, ignored the side reactions inside the lithium-ion battery, and assumed that the active material particles as single-sized spherical particles and the embedding and detachment of lithium ions occurred on the surface of the active material. The model has two dimensions, one in the direction of the radius of the active particles at the positive and negative electrodes and the other in the direction of the cell collector, positive and negative electrodes, and the thickness of the diaphragm [38].

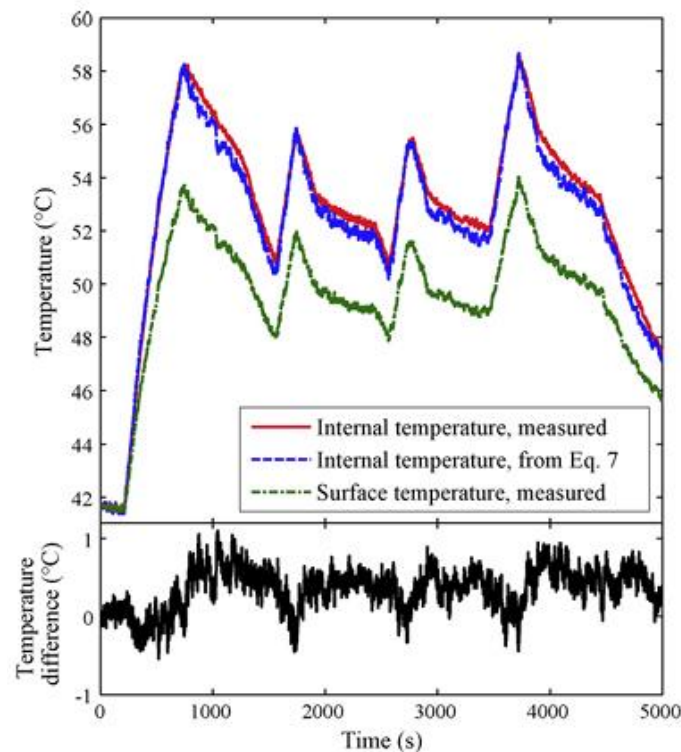


Figure 3. One-dimensional electrochemical model to obtain battery temperature results [96].

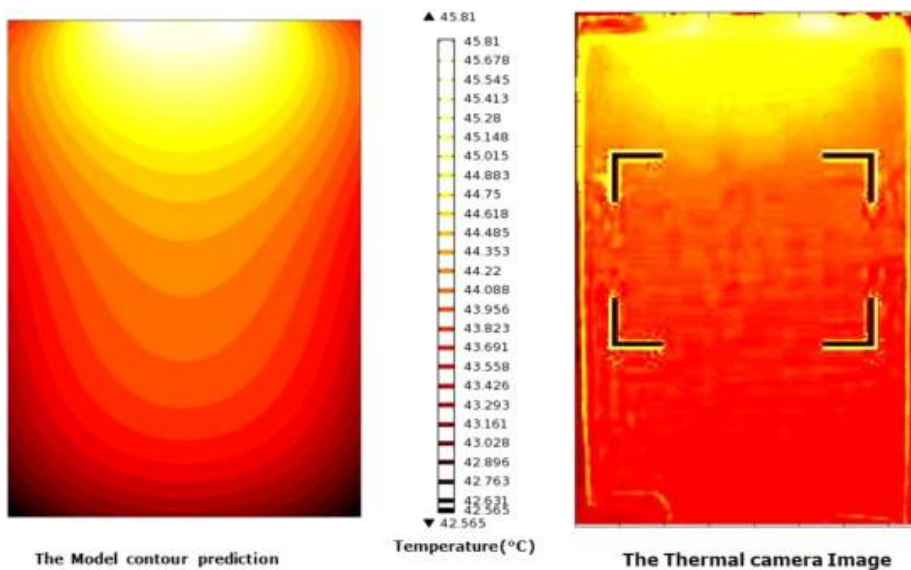


Figure 4. Two-dimensional electrochemical model to characterize the planar temperature diagram of lithium-ion battery [105].

Currently, the 2D model is the most widely used electrochemical model, but it can only predict the temperature change of the cell in the plane, while the 3D model can provide the most comprehensive information about the cell interior, including the microstructure of the electrodes and the multiscale transport process, but it also has the highest computational cost and model complexity. For the earlier study of 3D modeling [110], a 3D hierarchical model considering boundary radiative and convective heat transfer was developed by comparing 1D, 2D, and 3D models. Through validation, it was found that the accuracy of the three-dimensional model was significantly higher than the other models. For the discharge process of lithium iron phosphate batteries, ref. [111] developed a pseudo-3D electrochemical-thermal model to study the thermal and electrical behaviors of lithium-ion batteries during the discharge process. The battery is considered 3D, while the local battery cells are regarded as 1D, i.e., a homogeneity index is introduced to characterize the distribution of the SOCs among the 1D battery cells, thus simplifying the complexity of the 3D model. The authors of ref. [112] established a 3D electrochemical-thermal model to study, in detail, the thermal behavior of Li-ion batteries during discharge, especially analyzing the effects of discharge conditions such as current rate and ambient temperature on the thermal characteristics of the battery. The temperature distribution and potential distribution inside the battery were simulated using the finite element method, and the dynamic thermal behavior changes of the battery under different driving cycles were explored. The authors of ref. [37] coupled a P2D model with a 3D thermal model to simulate the 3D temperature distribution inside an 18650-type cylindrical battery. The temperature distribution at the end of charging and discharging is shown in Figure 5. It can be seen that the cell heat production is concentrated at the top and bottom of the cell. There is a large temperature gradient in the radial direction of the cell, and the temperature distribution is more uniform in the axial direction.

Therefore, each type of electrochemical model has its applicable scenarios and limitations. One-dimensional models are suitable for rapid analysis and preliminary design, while 2D and 3D models are better suited for more detailed battery design and optimization. As computational power and numerical methods continue to advance, 3D models are becoming increasingly widespread due to their ability to provide more accurate predictions of battery performance. When conducting a comprehensive analysis of battery thermal effects, it is essential to consider various factors that influence heat generation and dissipation within the battery, thereby achieving a more accurate analytical model.

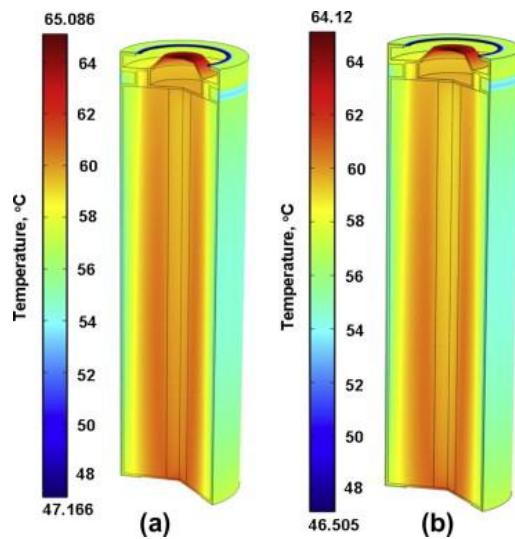


Figure 5. A three-dimensional electrochemical model to characterize the overall battery temperature diagram (a) charging and (b) discharging [37].

4.1.2. Based on the Equivalent Circuit Model

Equivalent circuit models decompose a battery into its thermal capacitance and thermal resistance and connect these components with electrical resistors and capacitors in the model. The potential in the circuit model reflects the temperature changes in the battery. For batteries where the material is assumed to be uniform and distributed evenly across the same layer, two common types of equivalent circuit models are used: the first-order and second-order equivalent circuit models. The first-order model represents the battery's overall thermal capacitance and resistance with a single set of capacitors and resistors, assuming the battery has a uniform temperature across its entirety. In contrast, the second-order model divides the battery's temperature into surface and core temperatures, using two sets of capacitors and resistors to represent the thermal capacitance and resistance of both the core and surface. Compared to the first-order model, the second-order model better captures more dynamic temperature variations in the battery, as illustrated in Figures 6 and 7.

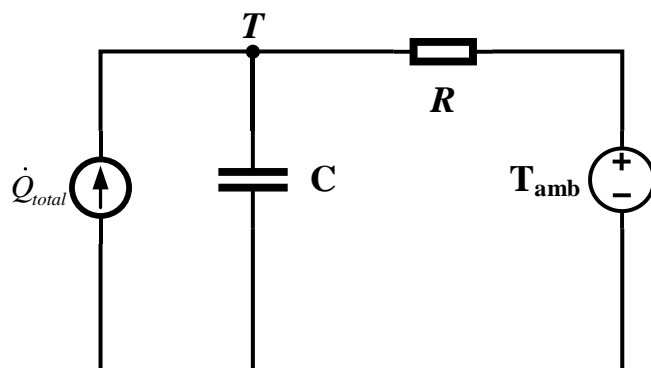


Figure 6. First-order thermal equivalent circuit model.

In Figure 6, T represents the battery's current temperature, T_{amb} denotes the ambient temperature, and R and C represent the overall thermal resistance and capacitance of the battery, respectively. This first-order model assumes uniform material distribution throughout the battery, making its parameters constant at any given moment. In contrast, Figure 7 illustrates the second-order thermal model, where T_c and T_s denote the core and surface temperatures of the battery, respectively. The convective thermal resistance R_u describes the convective cooling between the battery's surface temperature and the ambient temperature. R_c represents the conductive thermal resistance, which accounts

for the heat exchange between the battery core and its surface. C_c and C_s are the thermal capacitances for the battery core and surface, respectively. Typically, the model assumes uniform material properties within the battery, so the specific heat capacity is consistent at different internal locations.

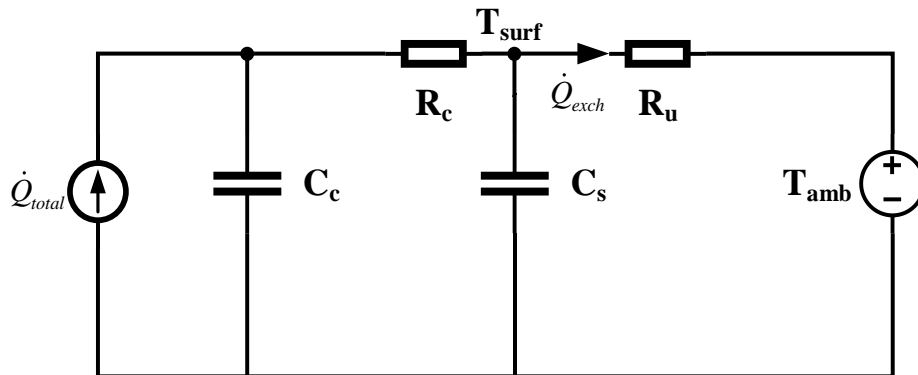


Figure 7. Second-order thermal equivalent circuit model.

Building on the two models discussed, they can be further categorized into lumped-parameter models and distributed-parameter models based on their complexity. Lumped-parameter models simplify the calculation process compared to detailed distributed models, thereby reducing computational costs. These efficient lumped thermal models use a single temperature input to capture model parameters [39]. When the battery system is integrated into a device, only a few lumped parameters are needed to effectively predict electrical performance and conduct detailed thermal analysis. Some researchers also use both the surface and core temperatures of the battery to develop lumped thermal models.

One major challenge with temperature prediction using equivalent circuit models for lithium-ion batteries is obtaining high-accuracy model parameters. For instance, ref. [113] combined a second-order equivalent circuit thermal model with a 2RC equivalent circuit model to propose a thermal model that considers the coupled effects of internal electrochemical reactions, temperature, and SOC. In this model, a particle swarm algorithm was used for offline identification of the thermal model, while a dual time-window method was employed for online identification of the 2RC equivalent circuit model. The identified model was then corrected using DUKF to achieve accurate estimates of SOC and battery temperature. Beyond offline identification methods, many thermal model identification approaches use various least-squares algorithms for online identification. For example, ref. [114] introduced the concept of a second-order thermal model and applied it to cylindrical lithium-ion batteries, using least-squares methods for parameter identification. Parameters obtained from this process were used to predict core and surface temperatures using Equation (10), facilitating health monitoring of the battery. Similarly, ref. [115] used least-squares methods to identify parameters for a second-order thermal model, utilizing surface temperature and voltage circuit changes as inputs for the identification process. In contrast, ref. [116] combined second-order and 2RC equivalent circuit thermal models but reduced the input parameters using only the surface temperature difference and heat generation calculated from Equation (8). They applied JKF to estimate the challenging-to-measure core temperature, improving adaptability to varying environmental temperatures. The authors of ref. [117] used a first-order RC equivalent circuit model for electrical modeling and employed a thermal model similar to the second-order model for heat analysis. They connected these models to capture the interaction between battery thermal and electrical behaviors, using EKF for temperature estimation. Similar to [117,118] also used a first-order RC model for the electrical characteristics part, but its improvement, based on the first-order thermal model, proposed that the thermal model is able to output the real-time average and maximum temperatures simultaneously. The proposed model was implemented in SPICE and compared with the FEM model, which ensures high accuracy and reduces the computation time at the same time. For estimating both internal and surface temperatures

of lithium-ion batteries, ref. [119] combined a temperature-dependent electrical model with a dual-state thermal model, using least-squares methods for joint identification and applying improved EKF for real-time temperature estimation. The authors of ref. [120] compared the effects of various least-squares algorithms (ULS, CLS, and WLS) on first-order thermal model identification, finding that WLS, which accounts for measurement noise, provided significant accuracy advantages. Although [121] also used a second-order thermal model, it did not predict internal and surface temperatures separately but rather used their average to estimate overall temperature in a two-dimensional space. Unlike conventional thermal models, ref. [122] did not use thermal equivalent circuit models but employed a second-order RC equivalent circuit model, developing a dynamic model based on SOC and battery temperature with linear spline functions for parameter dependency. To address the challenge of measuring entropy heat coefficients in Equation (8), ref. [123] proposed a fast continuous entropy coefficient identification method for the parameter identification of first-order thermal models, achieving lower time and equipment costs. To mitigate errors from sensor temperature data, ref. [124] designed an EKF to eliminate nonlinear biases and sensor errors in the second-order thermal model. In addition to temperature prediction, ref. [125] extended the second-order thermal model using Lyapunov analysis to design a nonlinear observer that incorporates surface temperature measurements and reconstructed core temperature output errors for monitoring thermal runaway. In ref. [101], the authors expanded the thermal model to represent the entire battery, rather than just a single plane, by simultaneously measuring both surface and internal temperatures to determine thermal transfer coefficients and thermal capacities, as shown in Figure 8. In addition to monitoring the battery cell, ref. [126] established a thermal model of a one-dimensional battery string, as shown in Figure 9. This model is based on the thermal model of a single cell and considers the thermal interaction between the battery cells, such as the heat conduction between adjacent cells and the thermal dynamics of the coolant flow. The uncertainty of the internal resistance of the battery cell is considered, and a robust observer is designed to reduce the worst-case estimation error caused by uncertainty.

$$\begin{cases} C_c \frac{dT_c}{dt} = Q + \frac{T_s - T_c}{R_c} \\ C_s \frac{dT_s}{dt} = \frac{T_f - T_s}{R_u} + \frac{T_s - T_c}{R_c} \end{cases} \quad (10)$$

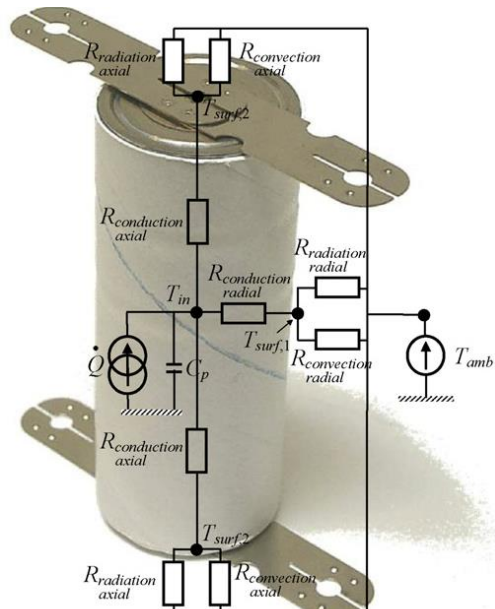


Figure 8. The extended thermal equivalent circuit model used to represent the temperature change of the battery plane [101].

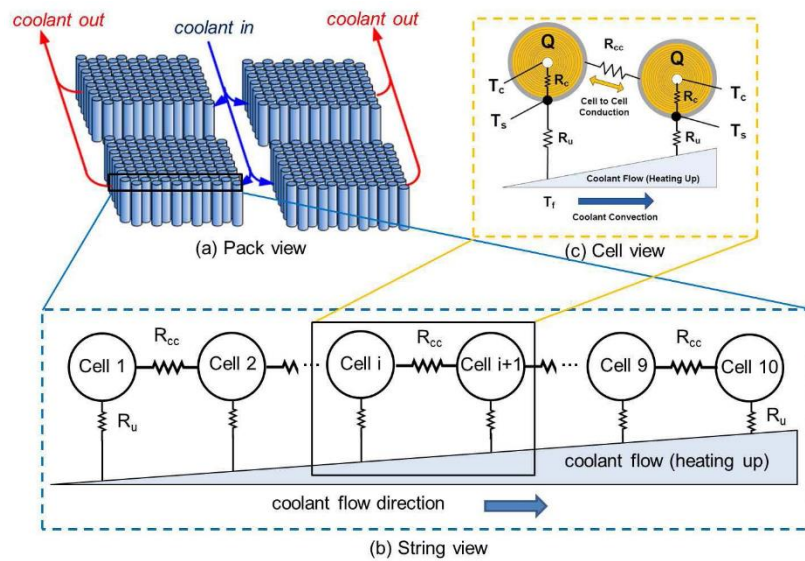


Figure 9. Thermal equivalent circuit model of battery pack extended by thermal equivalent circuit model [126].

In summary, the first step in using an equivalent circuit model approach is to establish the model. This involves predicting temperature using first-order and second-order thermal models or creating a thermoelectric coupling model to jointly predict temperature and electrical characteristics. After establishing the model, either online or offline identification methods are used to determine the parameters of the thermal equivalent model. Currently, the mainstream identification methods are various improved algorithms based on least squares. However, due to measurement deviations in inputs and difficulty in simulating the internal core temperature, there are still some errors when simulating battery temperature changes. Consequently, some studies incorporate Kalman filtering or similar algorithms for further prediction of the battery's internal core temperature after initial identification. A flowchart of the method for predicting battery temperature using the equivalent circuit model is shown in Figure 10.

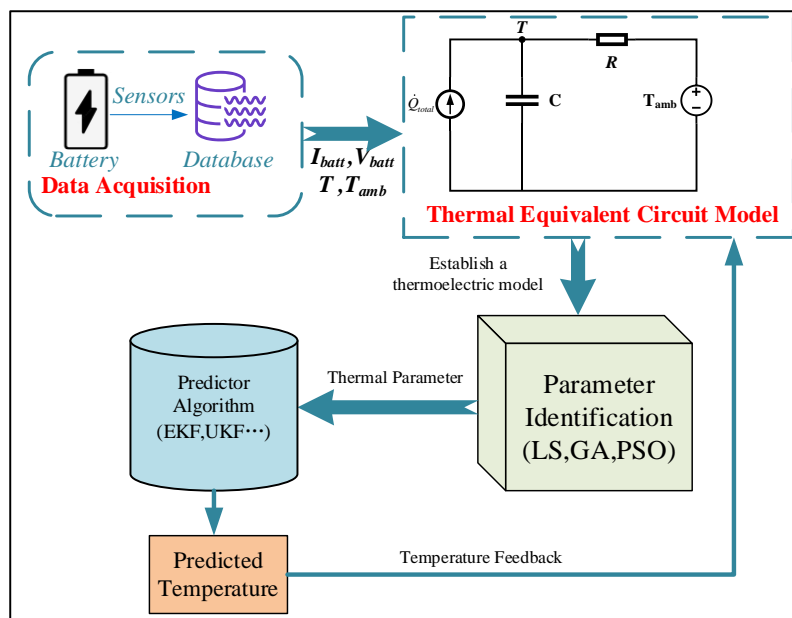


Figure 10. Predicting the temperature process framework of lithium-ion battery based on equivalent circuit model method.

4.1.3. Based on Electrochemical Impedance Method

In addition to the methods mentioned above, temperature changes during battery operation can affect the internal dynamics of lithium-ion batteries. These internal dynamics can be represented by EIS, establishing a relationship between electrochemical impedance (AC impedance) and internal temperature. Temperature prediction can then be achieved by measuring EIS-sensitive electrical parameters. This method does not damage the battery structure, responds quickly, and provides rich characterization information, making it widely applicable for temperature prediction. Various approaches exist for characterizing temperature using EIS-measured dynamic parameters. For example, ref. [127] initially used phase deviations between the excitation current and response voltage at a characteristic frequency of 40 Hz as a temperature-sensitive parameter for temperature prediction. In ref. [128], the authors used the real part of the electrochemical impedance at 10.3 kHz as the EIS temperature-sensitive parameter, discovering that different SOC could cause measurement errors up to 2.5 °C and that the temperature prediction range was limited to 0–25 °C. The authors of ref. [129] established a calibration relationship between impedance conductance at 215 Hz and the internal battery temperature and combined this with a thermal model to predict the internal temperature of the lithium-ion battery. It was found that using electrochemical impedance and impedance conductance for temperature characterization in the mid-frequency range limited the measurement range, making it unsuitable for high-temperature scenarios. To address this, ref. [130] developed a calibration relationship between the imaginary part of the electrochemical impedance at 300 Hz and temperatures above 68 °C and used piecewise linear fitting to extend the temperature prediction range to 95 °C. When the imaginary part of the impedance is zero, the corresponding excitation signal frequency is known as the cutoff frequency. Theoretical relationships between cutoff frequency and battery temperature can be established using the Arrhenius formula [131], but using cutoff frequency as a characterization parameter requires precise measurement of the excitation signal, which can be challenging in practice. According to ref. [128], the real part of the impedance is influenced by both temperature and SOC, whereas the imaginary part is less affected by temperature fluctuations and influenced by SOC. Thus, dividing the real part by the imaginary part of the electrochemical impedance can reduce the impact of SOC on temperature prediction results [132].

Apart from direct EIS measurements of dynamic parameters, some research has focused on simpler circuit methods based on these parameters for online temperature prediction. A direct approach involves replacing EIS instruments with an external excitation source and signal acquisition device. As shown in Figure 11, this method generates AC through the battery by opening and closing switches with a PDM signal. The AC voltage response of the battery can then be measured using an LPF. These signals are sampled, processed, and calculated to obtain EIS temperature-sensitive parameters for predicting the temperature of lithium-ion batteries [133]. To reduce the additional cost of external excitation sources, some researchers have proposed using DC/DC converters connected to the battery during operation to generate perturbation signals. By applying sinusoidal perturbations to the duty cycle of a Buck converter, the output DC is modulated with a sinusoidal disturbance signal, which can be used as an excitation signal for temperature prediction under constant current charging conditions [134]. Since the cutoff frequency varies with temperature, online temperature prediction based on cutoff frequency requires iterative algorithms to update the cutoff frequency corresponding to the current temperature. It is important to note that fluctuations in load-induced battery current can interfere with preset EIS excitation signals, making this method suitable only for constant current charge and discharge conditions. Additionally, active balancing circuits based on switched capacitors involve current surges during capacitor charge and discharge processes [135], which have been used to achieve the online resistance measurement of lithium-ion batteries. However, because the excitation source is the capacitor current during unbalanced states, this method is limited to temperature prediction for unbalanced batteries. Despite measuring various dynamic parameters of lithium-ion batteries and

establishing hidden relationships between temperature and related parameters, the high cost of EIS measurements, the potential impacts of different battery parameters on dynamic parameters, and the lack of universal EIS characteristics across different battery models still constrain the application of the EIS method. The following Table 1 provides a summary of the electrochemical impedance method.

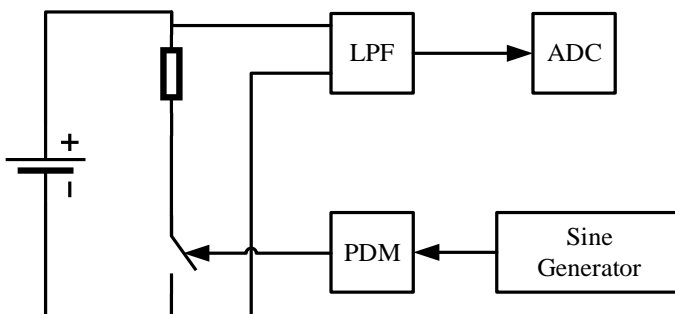


Figure 11. Schematic diagram of EIS measurement system using external excitation source and signal acquisition and processing device [133].

Table 1. Summary of electrochemical thermal modeling-based temperature estimation methods.

Reference	Types of Models	Article Contribution
Srinivasan et al. [127]	Online EIS measurement	Prediction of battery temperature based on the phase deviation between excitation current and response voltage at 40 Hz in EIS as a temperature-sensitive parameter.
Schmidt et al. [128]	Online EIS measurement	The real part of the electrochemical impedance at 10.3 kHz is used as the EIS temperature-sensitive electric parameter to predict the temperature, and the prediction range is limited to 0–25 °C under this method.
Richardson, Robert R., David A. Howey [129]	Online EIS measurement	Impedance conductance at 215 Hz combined with battery thermal modeling was collected to achieve temperature prediction of the inner core of a lithium-ion battery, which is not applicable to scenarios where high battery temperatures are required to be present in the prediction.
Spinner, Neil S., et al. [130]	Online EIS measurement	A calibration relationship between the imaginary part of the electrochemical impedance at 300 Hz and the temperature data above 68 °C was constructed and corrected using a segmented linear fit to expand the temperature prediction range up to 95 °C. The relationship between cutoff frequency and cell temperature can be established by the Arrhenius equation association, but it may be more difficult to realize in practical use.
Raijmakers, L. H. J., et al. [131]	Online EIS measurement	Dividing the real and imaginary parts of electrochemical impedance as a thermal parameter for temperature prediction can weaken the effect of SOC on the temperature prediction results.
Xiang et al. [132]	Online EIS measurement	

Table 1. Cont.

Reference	Types of Models	Article Contribution
Raijmakers, Luc HJ, et al. [133]	Replacement of EIS measurement instruments with external excitation sources and signal acquisition and processing units	Sinusoidal PDM signals simulate AC signals; LPF measures AC voltage response of batteries.
Hussein, Ala A., Abbas A. Fardoun. [134]	Replacement of EIS measurement instruments with external excitation sources and signal acquisition and processing units	A perturbation is applied to the duty cycle of the Buck converter, and this signal is used as the excitation signal.
Moral, Cristina Gonzalez et al. [135]	Replacement of EIS measurement instruments with external excitation sources and signal acquisition and processing units	Acquisition of the voltage response induced at the battery terminals with sudden current changes during the operation of the active equalization circuit of the switched capacitor.

4.2. Based on Data-Driven Method

During battery operation, various chemical reactions occur inside the battery. Traditional model-based methods represent these reactions through mathematical modeling. However, due to the complexity of the internal chemical reactions and the uncertainty of the battery's operating environment, such models often fail to fully capture the internal changes during battery operation. Additionally, in actual operations, the thermal behavior between the battery core and its surface differs significantly from the chemical reactions. Existing thermal models typically identify thermal parameters over a fixed period, which does not account for long-term temperature changes, particularly in larger-capacity batteries. As a result, data-driven methods have been widely applied to estimate the temperature of lithium-ion batteries. Learning from collected data, these methods uncover hidden relationships that improve temperature prediction. Compared to model-based methods, data-driven approaches can predict battery temperature more quickly, with better generalizability and portability. A schematic diagram of the data-driven temperature estimation approach is shown in Figure 12.

For data-driven prediction methods, constructing an appropriate neural network model and collecting a well-structured dataset are critical. For example, ref. [40] developed an ANN model to simulate the surface temperature of nickel–metal hydride batteries during charging. Later, ref. [41] extended this ANN-based temperature prediction method by creating a dual-layer ANN model to reduce errors in data collection. This model predicts battery voltage using collected current and SOC data, which is then used along with voltage, current, and SOC as inputs for temperature prediction. Additionally, ref. [42] proposed a dynamic ANN method based on the NARX model to analyze the thermal behavior of lithium-ion batteries. The network was trained using the Levenberg–Marquardt backpropagation algorithm with discharge voltage and temperature as inputs and outputs. Beyond basic ANN models, RNNs are widely used in temperature prediction due to their ability to retain and forget information in time-series data, which allows them to effectively consider the influence of previous battery parameters. In ref. [136], the authors applied this recurrent structure to LSTM and GRU networks to predict the surface temperature of lithium-ion batteries during discharge at various environmental temperatures. Meanwhile, ref. [137] compared FNNs with LSTM-based RNNs and found that LSTM-based models perform better in estimating temperature under varying environmental conditions, even at lower temperatures. LSTM networks connect short-term memory to capture long-term memory features, making them well-suited for handling the time dependency of temperature changes, as the thermodynamics of batteries are governed by time-dependent differential equations. The authors of ref. [138] proposed an LSTM-based method combined with stretch-forward techniques to monitor the deviation of predicted temperatures and detect thermal faults in lithium-ion batteries in real time. In ref. [139], the authors applied

the EGA to obtain the optimal segmentation strategy for temperature time-series data and combined it with a BiLSTM network. This method predicts the highest and lowest temperatures in energy storage station battery packs. Additionally, an improved loss function was employed to enhance model accuracy. Ablation experiments confirmed that the EGA-BiLSTM-based short-term temperature prediction model exhibits strong predictive capability. Gated recurrent units (GRUs) are a variant of LSTM networks. GRUs combine the forget and input gates into a single update gate while adding a reset gate and merging cell and hidden states. This design leads to faster training speeds than LSTM. The authors of ref. [140] developed a GRU-RNN model and improved data normalization methods using actual battery data to enhance the accuracy and robustness of predictions. In ref. [141], the authors used a TSIA to optimize an RBF neural network for predicting the internal temperature of lithium-ion batteries and filtered abnormal values in the RBF model predictions using an EKF, leading to more precise temperature estimates. In conclusion, data-driven temperature prediction methods offer better computational efficiency and simpler implementation. However, the complexity of data collection during training makes it difficult to apply these methods in practical use. The following Table 2 provides a summary of the data-driven approach.

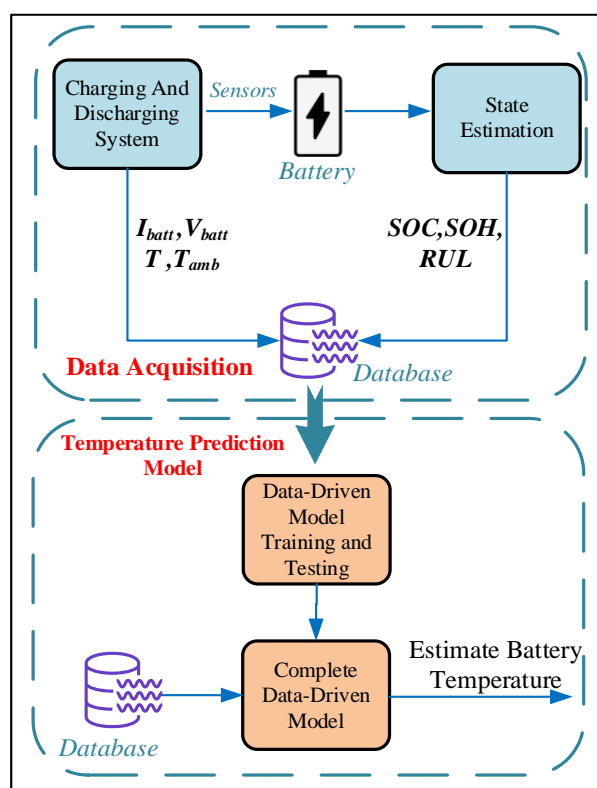


Figure 12. Prediction of lithium-ion battery temperature flowchart based on model and data-driven combination method.

Table 2. Summary of data-driven-based temperature estimation method.

Reference	Types of Models	Article Contribution
Fang et al. [40]	ANN model	ANN was used to predict different charging and discharging rates at different ambient temperatures.
Hussein, Ala A [41]	Dual-layer ANN model	A two-layer ANN model was constructed, and the collected data were used to predict the voltage of the battery, and then the predicted data were used to predict the temperature change of the battery.

Table 2. *Cont.*

Reference	Types of Models	Article Contribution
Jamshidi, Mohammad Behdad, and Safdar Rostami [42]	NARX- ANN model	A nonlinear autoregressive exogenous (NARX)-based model is proposed to train the network using the Levenberg–Marquardt backpropagation algorithm.
Jiang et al. [136]	LSTM/GRU	LSTM and GRU, variants of RNN, were used for temperature prediction.
Naguib et al. [137]	FNN and LSTM	Comparison of the advantages and disadvantages of FNN and LSTM in predicting time-series lithium-ion battery temperature variations.
Ojo et al. [138]	Stretch-forward LSTM	An LSTM model incorporating stretch-forward is proposed for the battery temperature.
Jiang et al. [139]	EGA- BiLSTM	Optimal segmentation strategy of time-series data on temperature obtained by EGA, combined with BiLSTM to realize high-precision temperature prediction of batteries in energy storage power plants
Yao, Qi, Dylan Dah-Chuan Lu, and Gang Lei [140]	GRU-RNN	Proposes an improved data normalization method based on actual data collected from batteries to improve the accuracy of GRU-RNN estimation.
Liu et al. [141]	TSIA-RBF-EKF	Temperature prediction using TSIA-optimized RBF and filtering the predicted values by EKF.

4.3. Combination of Model and Data-Driven Methods

Due to the limitations of model-based prediction methods and the challenges of data collection for data-driven approaches, some research has begun to explore hybrid methods that combine models with data-driven techniques to predict lithium-ion battery temperature changes. These studies often base their approach on a thermal behavior model of the battery, using the model's output as input data for the data-driven component. For example, ref. [43] developed a hybrid model that employs a time/space separation method to design a spatiotemporal distribution model for calculating battery temperature, and it integrates a data-driven neural network to compensate for mismatches between the model and calculated temperature caused by spatial nonlinearity and other model uncertainties. In ref. [142], the EKF is used to predict battery temperature changes based on an identified second-order thermal equivalent circuit model. A neural network is employed to represent the noise in the battery model, and particle swarm optimization is used to dynamically adjust the noise covariance in the EKF, compensating for the model noise. In ref. [143], a second-order RC circuit model is used to simulate the electrical characteristics of the battery. The simulated voltage and current are input into a heat generation model, which calculates heat generation to feed into a second-order thermal equivalent circuit model for core and surface temperature simulations. These simulated values are then fed into a 2D GLSTM neural network, resulting in a model capable of real-time prediction of both surface and core temperatures of lithium-ion batteries. Beyond models based on heat generation, ref. [144] developed an ETNN model. In this approach, a simplified single-particle model represents the battery's electrochemical reactions, while a lumped thermal model represents its thermal behavior. The outputs from these models are used as inputs to a neural network for joint estimation of the SOC and core temperature of lithium-ion batteries. In ref. [145], a combination of EIS and a second-order RC equivalent circuit model is used as input to an artificial neural network classifier to predict the SOT of lithium-ion batteries during operation. Beyond the hybrid model and data-driven approaches mentioned, another type of combined method uses PINNs to predict battery temperature changes. PINNs are designed to solve PDEs, which align well with the heat generation model of lithium-

ion batteries. In ref. [146], the authors utilized PINN to solve the heat generation model, combining real battery test data with a thermal relationship model for lithium-ion batteries. The model is optimized by adjusting the coefficients in the loss function. In [147], PINNs were combined with LSTM networks. LSTM is used to predict surface temperatures at different locations within a battery pack, and these predictions serve as inputs to the PINN model, enhancing the accuracy of temperature predictions. In summary, hybrid methods combining model-based and data-driven approaches typically merge the accuracy of physical models with the generalization capabilities of data-driven methods to improve the accuracy and robustness of battery temperature estimation. This fusion allows better compensation for model noise and enhances performance across various environments and operational conditions. Moreover, this combined approach shows great promise for practical applications. The following Table 3 provides a summary of the combination of model and data-driven method.

Table 3. Summary of combination of model and data-driven temperature estimation methods.

Reference	Types of Models	Article Contribution
Liu, Li [43]	Physical model + feed-forward back-propagation neural network	Design of a spatiotemporal distribution model using a time/space separation approach and incorporating a data-based neural network model to compensate for model-computed temperature mismatches.
Liu et al. [142]	Equivalent circuit model + EKF + NN	Uses an EKF to predict temperature variations in batteries and a neural network to characterize battery model noise.
Surya et al. [143]	Equivalent circuit model + 2-D GLSTM	The battery electrical characteristics are simulated over a second-order RC circuit model, and the simulations are fed into a 2-D-GLSTM neural network for training and real-time prediction of surface and inner temperatures of lithium-ion batteries.
Feng et al. [144]	ETNN	A simplified single-particle model is used to characterize the thermal behavior of the battery, and the output simulations of the model are used as inputs to the neural network to estimate the SOC and core temperature of the lithium-ion battery.
Vaidya et al. [145]	EIS + equivalent circuit model + ANN	A combination of (EIS) and 2nd-order RC equivalent circuit models are used as inputs to the ANN to predict the temperature of lithium-ion batteries.
Cho et al. [146]	PINN	A PINN pair-generated thermal model is solved using PINN and optimized by combining battery test data with a thermal model of a lithium-ion battery.
Cho et al. [147]	PINN + LSTM	An LSTM is used to predict the surface temperatures at different locations within the battery pack, and these predictions are used as inputs to the PINN model.

5. Problems with Current Research and Discussion

According to the above analysis of the temperature characteristics of lithium-ion batteries and the discussion of various types of temperature prediction methods, we find that for the current temperature prediction methods for lithium-ion batteries, model-based methods are mainly analyzed according to their different characteristics, for example, methods based on electrochemical models with a focus on analyzing the chemical properties of the battery as a whole; methods based on equivalent circuits are more biased to the thermal parameters of the battery; and the electrical components are related to the electrical characteristics. For example, electrochemical model-based methods focus on analyzing the overall chemical properties of the battery; equivalent circuit-based methods are more oriented to relate the thermal parameters of the battery to the electrical components and the electrical properties of the battery. Although the accuracy of these model-based methods

has been quite impressive, there are still some errors that are difficult to resolve, which may be due to the fact that most of the model-based methods are based on a certain property of the battery, resulting in a lack of description of the thermal behavior of the battery. In addition, the accuracy of the battery model is crucial for temperature estimation. However, the chemical and physical processes of lithium-ion batteries are very complex, including electrochemical reactions, thermal effects, battery aging, etc., which may affect the accurate estimation of temperature. This direction of representing the thermal behavior of the battery in a mathematical model can also hardly avoid the existence of errors due to mathematical equations. In addition, the time required by different models to predict the temperature process in the model-based approach is also an issue that needs to be considered in practical applications. The electrochemical-based approach has a significantly higher computing time than the equivalent circuit model-based approach due to the characterization of the temperature at different orientations of the cell. The EIS method, which is usually a static measurement, is difficult to compare.

In contrast, the data-driven approach avoids this error due to the lack of attribute characterization of the battery, and it automatically obtains the implicit relationship between various parameters of the battery and the battery temperature by training the input data with various types of data-driven models, which is less computationally burdensome and easier to implement than the model approach. However, data-driven methods require a large amount of data for training, and in the process of collecting data under various operating conditions of the battery, in order not to damage the structure of the battery, a non-intrusive measurement method may introduce errors. At the same time, there may also be a cumulative error in the collection process, which affects the accuracy of the temperature estimation.

The model-based and data-driven temperature prediction methods are neutralized, and although the above two problems are solved, the establishment of such a highly accurate temperature estimation model requires a large amount of computational resources in the model-based part, which may be a limitation for a real-time temperature monitoring system, and results in the high cost of this method in actual operation, which makes it difficult to be put into real use.

Also, the prediction times of data-driven models, as well as data-driven fusion models, are difficult to determine, influenced by the hyperparameters chosen for the training of the models built and the complexity of the dataset collected by the battery.

In addition, most of the various types of models currently established focus only on a single battery individual, while different types of lithium-ion batteries (e.g., lithium iron phosphate, lithium ternary, etc.) have different thermal characteristics. How to also design generalized temperature estimation models for different types of batteries is a problem. The purpose of predicting the temperature process of lithium-ion batteries is to better observe the temperature state of the battery in order to achieve the best performance and prevent the battery from thermal runaway, so it may be necessary to collect the relevant thermal runaway data, and the thermal runaway process, which is an extremely fast and dangerous process, is difficult to conduct for experiments and collection purposes.

Therefore, in order to solve the above problems, the first need is to solve the problem of excessive errors in the sensor acquisition process. As the use of high-precision sensors does not seem to be a good move, perhaps various filtering algorithms can be used to reduce the noise interference in the acquisition process. For the model-based approach, in order to solve the singularity in its characterization, perhaps a joint model approach can be adopted, using multiple models to provide parameters to each other for error control, to achieve high-precision temperature prediction. For the data-driven approach, it may be possible to first screen the input parameters of the model and select parameters with higher relevance for temperature prediction; in addition, for the input data, more typical datasets could be selected to try to make the adopted datasets cover more of the various phenomena that may occur in the battery operation process. Table 4 summarizes the existing issues, challenges, and recommendations for future research for the research community.

Table 4. Summary of major issues, challenges, and research recommendations.

Strategy	Major Issues and Challenges	Future Research Recommendations
Based on electrochemical model	<ul style="list-style-type: none"> ◆ Arithmetic burden and long simulation time due to high precision results; ◆ Cannot be embedded in a real BMS; ◆ Theoretical complexity of electrochemical modeling makes it difficult to put it into use by the public; ◆ Requires a lot of experiments to determine the battery characteristics; ◆ Difficult to build adaptive models in practical use. 	<ul style="list-style-type: none"> ◆ Attempt to reduce modeling complexity and computational costs; ◆ Due to its high accuracy results, try it as a validation model for other models; ◆ To adapt to changes in chemical parameters of the battery, try to build adaptively.
Based on the equivalent circuit model	<ul style="list-style-type: none"> ◆ Easier to implement in experimental environments, but a large amount of data can lead to model arithmetic overload under long working conditions; ◆ Noise from external measurements affects the accuracy of the results; ◆ The thermal parameters are not considered in conjunction with the electrochemical model, which may lead to errors in model accuracy; ◆ Some model complexity was sacrificed for practical use versus computing time, limiting the results of predicted temperatures. 	<ul style="list-style-type: none"> ◆ Build models that can be switched between model complexity and model details based on real-world usage; ◆ Develop high-precision adaptive parameter models that can be adapted to a variety of batteries and operating conditions; ◆ Combine the method with other models to obtain an easier-to-implement method.
Based on electrochemical impedance method	<ul style="list-style-type: none"> ◆ Prediction of impedance by temperature change is difficult to realize with on-line measurements due to its need for static testing; ◆ At the same time, small temperature variations have small changes in impedance, and determining the temperature change for such small variations is very difficult; ◆ This method usually requires extensive experimentation and is difficult to use in practice. 	<ul style="list-style-type: none"> ◆ Build a smaller impedance measurement system and evaluate the possibility of using this method in a BMS; ◆ Determine how the results will be judged for accuracy in practical applications; ◆ Develop impedance testing based on the system's power equipment, rather than using specific EIS experiments.
Based on data-driven method	<ul style="list-style-type: none"> ◆ In order to obtain higher accuracy, the computational cost of data-driven-based methods increases with the number of high-volume data and feature vectors, and the continuous accumulation of such data adds a great burden to the experimental process as well as to practical use; ◆ Since data-driven methods require training on the collected data, the ever-refined development of complex algorithms and the increasing computational time make it difficult to use this method in BMSs, and the research currently invested in this area is minimal; ◆ Data acquisition typically requires external measurements from physical sensors as feedback for online parameter tuning and, therefore, remains subject to acquisition data errors. 	<ul style="list-style-type: none"> ◆ Battery characteristics can be highly influenced by temperature, aging, and other uncertainties, so further research on adaptive modeling is recommended; ◆ Through proper design, simplify or design specific algorithms that make it possible to implement them in a BMS; ◆ An attempt can be made to investigate the more novel sensorless temperature estimation methods available.
Combination of model and data-driven prediction	<ul style="list-style-type: none"> ◆ The unavoidable accuracy errors in the model-based approach are further transferred into the data-driven part, resulting in the accumulation of errors in the prediction process; ◆ The high-accuracy model-based approach and the data-driven approach require large arithmetic power, and the computational burden of the combination of the two is even larger and more difficult to realize in a BMS. 	<ul style="list-style-type: none"> ◆ Highly accurate models or multi-model concatenation should be used to minimize the impact of model errors on the data-driven part; ◆ For practical use, the fusion model complexity and accuracy need to be balanced to ensure its feasibility for practical use in a BMS.

6. Conclusions

Lithium-ion battery temperature prediction is crucial for enhancing the performance and safety of electric vehicles. This paper systematically classifies and analyzes existing battery temperature prediction methods based on the temperature characteristics of lithium-ion batteries, considering how different temperatures affect battery mechanisms. The advantages and limitations of various methods are identified, leading to the conclusion that accurate temperature estimation is vital for battery thermal management, safe operation, and maximizing battery efficiency. Relying solely on sensors for temperature monitoring is impractical due to the inevitable measurement errors, significant limitations in monitoring the core temperature within the battery, and the high cost of measuring the temperature across the entire battery pack. Therefore, it is necessary to develop effective temperature estimation methods that can achieve high accuracy, adaptability, real-time estimation, feasibility of the overall model, cost-effectiveness, and distributed temperature estimation across the battery. Currently, battery temperature variations are primarily described using heat generation and heat transfer models. Based on these temperature expression methods, various approaches are used to monitor temperature changes in lithium-ion batteries. Depending on the modeling or characterization techniques, existing temperature estimation methods can be categorized into three types: model-based, data-driven, and hybrid methods, which combine both approaches. Model-based methods can be further divided into electrochemical models, equivalent circuit models, and electrochemical impedance spectroscopy-based models. Among these, electrochemical methods offer relatively high accuracy but are computationally intensive, making them challenging to implement in practical applications. Equivalent circuit models, while less accurate, are more practical for real-world use due to their flexibility in being simplified or expanded as needed. EIS-based methods do not require additional measurement data but depend on external excitation devices, making real-time temperature monitoring difficult. Data-driven methods, on the other hand, exhibit good generalization and computational efficiency but require large amounts of data and may lack a deep understanding of the underlying physical processes. Therefore, combining model-based and data-driven approaches—leveraging the accuracy of physical models and the generalization capabilities of data-driven methods—may become a key direction for the future development of battery temperature prediction technology. Furthermore, with the advancement of computational technologies and the application of new algorithms, such as neural networks and deep learning, the accuracy and efficiency of battery temperature prediction will continue to improve. Future research should focus more on predicting battery temperature under real-world operating conditions and optimizing prediction models for real-time application in battery management systems.

Funding: This research was funded by the Major Science and Technology Projects in Zhejiang Province—Key R & D Projects [2023C01SA301767].

Conflicts of Interest: The authors declare no conflict of interest.

References

1. Wada, M. Research and development of electric vehicles for clean transportation. *J. Environ. Sci.* **2009**, *21*, 745–749. [[CrossRef](#)] [[PubMed](#)]
2. Harding, G. Electric vehicles in the next millennium. *J. Power Sources* **1999**, *78*, 193–198. [[CrossRef](#)]
3. Chau, K.; Wong, Y. Hybridization of energy sources in electric vehicles. *Energy Convers. Manag.* **2001**, *42*, 1059–1069. [[CrossRef](#)]
4. Eaves, S.; Eaves, J. A cost comparison of fuel-cell and battery electric vehicles. *J. Power Sources* **2004**, *130*, 208–212. [[CrossRef](#)]
5. Nykvist, B.; Olsson, O. The feasibility of heavy battery electric trucks. *Joule* **2021**, *5*, 901–913. [[CrossRef](#)]
6. Cano, Z.P.; Banham, D.; Ye, S.; Hintennach, A.; Lu, J.; Fowler, M.; Chen, Z. Batteries and fuel cells for emerging electric vehicle markets. *Nat. Energy* **2018**, *3*, 279–289. [[CrossRef](#)]
7. Schmuck, R.; Wagner, R.; Hörpel, G.; Placke, T.; Winter, M. Performance and cost of materials for lithium-based rechargeable automotive batteries. *Nat. Energy* **2018**, *3*, 267–278. [[CrossRef](#)]
8. Blomgren, G.E. The development and future of lithium-ion batteries. *J. Electrochem. Soc.* **2016**, *164*, A5019–A5025. [[CrossRef](#)]
9. Goodenough, J.B. Evolution of strategies for modern rechargeable batteries. *Acc. Chem. Res.* **2012**, *46*, 1053–1061. [[CrossRef](#)]

10. Väyrynen, A.; Salminen, J. Lithium ion battery production. *J. Chem. Thermodyn.* **2012**, *46*, 80–85. [[CrossRef](#)]
11. Ji, Y.; Zhang, Y.; Wang, C.-Y. Li-ion cell operation at low temperatures. *J. Electrochem. Soc.* **2013**, *160*, A636–A649. [[CrossRef](#)]
12. Jilte, R.D.; Kumar, R.; Ma, L. Thermal performance of a novel confined flow Li-ion battery module. *Appl. Therm. Eng.* **2019**, *146*, 1–11. [[CrossRef](#)]
13. Ramadass, P.; Haran, B.; White, R.; Popov, B.N. Capacity fade of Sony 18650 cells cycled at elevated temperatures. *J. Power Sources* **2002**, *112*, 614–620. [[CrossRef](#)]
14. Zhang, Y.; Wang, C.-Y.; Tang, X. Cycling degradation of an automotive LiFePO₄ lithium-ion battery. *J. Power Sources* **2010**, *196*, 1513–1520. [[CrossRef](#)]
15. Shim, J.; Kostecki, R.; Richardson, T.; Song, X.; Striebel, K. Electrochemical analysis for cycle performance and capacity fading of a lithium-ion battery cycled at elevated temperature. *J. Power Sources* **2002**, *112*, 222–230. [[CrossRef](#)]
16. Spotnitz, R.; Franklin, J. Abuse behavior of high-power, lithium-ion cells. *J. Power Sources* **2003**, *113*, 81–100. [[CrossRef](#)]
17. Wang, Q.; Ping, P.; Zhao, X.; Chu, G.; Sun, J.; Chen, C. Thermal runaway caused fire and explosion of lithium ion battery. *J. Power Sources* **2012**, *208*, 210–224. [[CrossRef](#)]
18. Manas, M.; Yadav, R.; Dubey, R.K. Designing a battery Management system for electric vehicles: A congregated approach. *J. Energy Storage* **2023**, *74*, 109439. [[CrossRef](#)]
19. Surya, S.; Samanta, A.; Marcis, V.; Williamson, S. Smart core and surface temperature estimation techniques for health-conscious lithium-ion battery management systems: A model-to-model comparison. *Energies* **2022**, *15*, 623. [[CrossRef](#)]
20. Malik, M.; Mathew, M.; Dincer, I.; Rosen, M.; McGrory, J.; Fowler, M. Experimental investigation and thermal modelling of a series connected LiFePO₄ battery pack. *Int. J. Therm. Sci.* **2018**, *132*, 466–477. [[CrossRef](#)]
21. Surya, S.; Marcis, V.; Williamson, S. Core temperature estimation for a lithium ion 18650 cell. *Energies* **2020**, *14*, 87. [[CrossRef](#)]
22. Tanim, T.R.; Rahn, C.D.; Wang, C.Y. State of charge estimation of a lithium ion cell based on a temperature dependent and electrolyte enhanced single particle mode. *Energy* **2015**, *80*, 731–739. [[CrossRef](#)]
23. Farmann, A.; Sauer, D.U. A study on the dependency of the open-circuit voltage on temperature and actual aging state of lithium-ion batteries. *J. Power Sources* **2017**, *347*, 1–13. [[CrossRef](#)]
24. Guo, Z.; Xu, J.; Wang, X.; Mei, X. Fast multilayer temperature distribution estimation for lithium-ion battery pack. *eTransportation* **2023**, *18*, 100266. [[CrossRef](#)]
25. Beelen, H.; Shivakumar, K.M.; Rajmakers, L.; Donkers, M.C.F.; Bergveld, H.J. Towards impedance-based temperature estimation for Li-ion battery packs. *Int. J. Energy Res.* **2020**, *44*, 2889–2908. [[CrossRef](#)]
26. Alcock, K.M.; González-Vila, Á.; Beg, M.; Vedreño-Santos, F.; Cai, Z.; Alwis, L.S.M.; Goh, K. Individual cell-level temperature monitoring of a lithium-ion battery pack. *Sensors* **2023**, *23*, 4306. [[CrossRef](#)]
27. Richardson, R.R.; Ireland, P.T.; Howey, D.A. Battery internal temperature estimation by combined impedance and surface temperature measurement. *J. Power Sources* **2014**, *265*, 254–261. [[CrossRef](#)]
28. Wei, Z.; Zhao, J.; He, H.; Ding, G.; Cui, H.; Liu, L. Future smart battery and management: Advanced sensing from external to embedded multi-dimensional measurement. *J. Power Sources* **2021**, *489*, 229462. [[CrossRef](#)]
29. Rajmakers, L.; Danilov, D.; Eichel, R.-A.; Notten, P. A review on various temperature-indication methods for Li-ion batteries. *Appl. Energy* **2019**, *240*, 918–945. [[CrossRef](#)]
30. Ma, S.; Jiang, M.; Tao, P.; Song, C.; Wu, J.; Wang, J.; Deng, T.; Shang, W. Temperature effect and thermal impact in lithium-ion batteries: A review. *Prog. Nat. Sci. Mater. Int.* **2018**, *28*, 653–666. [[CrossRef](#)]
31. Nascimento, M.; Novais, S.; Ding, M.S.; Ferreira, M.S.; Koch, S.; Passerini, S.; Pinto, J.L. Internal strain and temperature discrimination with optical fiber hybrid sensors in Li-ion batteries. *J. Power Sources* **2018**, *410–411*, 1–9. [[CrossRef](#)]
32. Sun, B.; Xu, G.; Ji, X.; Yang, Z.; Guan, C.; Chen, S.; Chen, X.; Ma, Y.; Yu, Y.; Feng, J. A strain-resistant flexible thermistor sensor array based on CNT/MXene hybrid materials for lithium-ion battery and human temperature monitoring. *Sens. Actuators A Phys.* **2024**, *368*, 115059. [[CrossRef](#)]
33. Koshkouei, M.J.; Saniee, N.F.; Barai, A. Thermocouple selection and its influence on temperature monitoring of lithium-ion cells. *J. Energy Storage* **2024**, *92*, 112072. [[CrossRef](#)]
34. Yang, L.; Li, N.; Hu, L.; Wang, S.; Wang, L.; Zhou, J.; Song, W.-L.; Sun, L.; Pan, T.-S.; Chen, H.-S.; et al. Internal field study of 21700 battery based on long-life embedded wireless temperature sensor. *Acta Mech. Sin.* **2021**, *37*, 895–901. [[CrossRef](#)]
35. Kunze, P.; Greulich, J.M.; Tummaliyah, A.; Wirtz, W.; Hoeffler, H.; Woehrle, N.; Glunz, S.; Rein, S.; Demant, M. Contactless Inline IV Measurement of Solar Cells Using an Empirical Model. *Sol. RRL* **2022**, *7*, 2200599. [[CrossRef](#)]
36. Wang, L.; Lu, D.; Song, M.; Zhao, X.; Li, G. Instantaneous estimation of internal temperature in lithium-ion battery by impedance measurement. *Int. J. Energy Res.* **2019**, *44*, 3082–3097. [[CrossRef](#)]
37. Saw, L.; Ye, Y.; Tay, A. Electrochemical–thermal analysis of 18650 Lithium Iron Phosphate cell. *Energy Convers. Manag.* **2013**, *75*, 162–174. [[CrossRef](#)]
38. Doyle, M.; Fuller, T.F.; Newman, J. Modeling of galvanostatic charge and discharge of the lithium/polymer/insertion cell. *J. Electrochem. Soc.* **1993**, *140*, 1526–1533. [[CrossRef](#)]
39. Mahamud, R.; Park, C. Reciprocating air flow for Li-ion battery thermal management to improve temperature uniformity. *J. Power Sources* **2011**, *196*, 5685–5696. [[CrossRef](#)]
40. Fang, K.; Mu, D.; Chen, S.; Wu, B.; Wu, F. A prediction model based on artificial neural network for surface temperature simulation of nickel–metal hydride battery during charging. *J. Power Sources* **2012**, *208*, 378–382. [[CrossRef](#)]

41. Hussein, A.A. A sensorless surface temperature measurement method for batteries using artificial neural networks. In Proceedings of the 2018 IEEE Energy Conversion Congress and Exposition (ECCE), Portland, OR, USA, 23–27 September 2018. [CrossRef]
42. Jamshidi, M.B.; Rostami, S. A dynamic artificial neural network approach to estimate thermal behaviors of li-ion batteries. In Proceedings of the 2017 IEEE 2nd International Conference on Automatic Control and Intelligent Systems (I2CACIS), Kota Kinabalu, Malaysia, 21 October 2017. [CrossRef]
43. Liu, Z.; Li, H.-X. A spatiotemporal estimation method for temperature distribution in lithium-ion batteries. *IEEE Trans. Ind. Inform.* **2014**, *10*, 2300–2307. [CrossRef]
44. Bezsonov, I.I.; Waller, G.H.; Ko, J.; Nadimpalli, S.P.V. In operando measurement of surface strain of 18650 Li-ion cells during cycling. *J. Power Sources* **2024**, *592*, 233915. [CrossRef]
45. He, D.; Wang, J.; Peng, Y.; Li, B.; Feng, C.; Shen, L.; Ma, S. Research advances on thermal runaway mechanism of lithium-ion batteries and safety improvement. *Sustain. Mater. Technol.* **2024**, *41*, e01017. [CrossRef]
46. Wang, Q.; Jiang, B.; Li, B.; Yan, Y. A critical review of thermal management models and solutions of lithium-ion batteries for the development of pure electric vehicles. *Renew. Sustain. Energy Rev.* **2016**, *64*, 106–128. [CrossRef]
47. Börger, A.; Mertens, J.; Wenzl, H. Thermal runaway and thermal runaway propagation in batteries: What do we talk about? *J. Energy Storage* **2019**, *24*, 100649. [CrossRef]
48. Song, L.; Li, L.; Xiao, Z.; Zhang, J.; Cao, Z.; Zhou, Q.; Hu, C.; Liu, J. Estimation of temperature distribution of LiFePO₄ lithium ion battery during charge–discharge process. *Ionics* **2016**, *22*, 1517–1525. [CrossRef]
49. Song, M.; Hu, Y.; Choe, S.-Y.; Garrick, T.R. Analysis of the heat generation rate of lithium-ion battery using an electrochemical thermal model. *J. Electrochem. Soc.* **2020**, *167*, 120503. [CrossRef]
50. Zhao, D.; Chen, W. Analysis of polarization and thermal characteristics in lithium-ion battery with various electrode thicknesses. *J. Energy Storage* **2023**, *71*, 108159. [CrossRef]
51. Zhang, G.; Chen, S.; Zhu, J.; Dai, H.; Wei, X. Investigation on the impact of high-temperature calendar and cyclic aging on battery overcharge performance. *SAE Int. J. Adv. Curr. Pract. Mobil.* **2022**, *4*, 1953–1960. [CrossRef]
52. Zhang, X. Thermal analysis of a cylindrical lithium-ion battery. *Electrochim. Acta* **2011**, *56*, 1246–1255. [CrossRef]
53. Bernardi, D.; Pawlikowski, E.; Newman, J. A general energy balance for battery systems. *J. Electrochem. Soc.* **1985**, *132*, 5–12. [CrossRef]
54. Xiao, Z.; Liu, C.; Zhao, T.; Kuang, Y.; Yin, B.; Yuan, R.; Song, L. Review—Online Monitoring of Internal Temperature in Lithium-Ion Batteries. *J. Electrochem. Soc.* **2023**, *170*, 057517. [CrossRef]
55. Wang, C.-J.; Zhu, Y.-L.; Gao, F.; Bu, X.-Y.; Chen, H.-S.; Quan, T.; Xu, Y.-B.; Jiao, Q.-J. Internal short circuit and thermal runaway evolution mechanism of fresh and retired lithium-ion batteries with LiFePO₄ cathode during overcharge. *Appl. Energy* **2022**, *328*, 120224. [CrossRef]
56. Jiaqiang, E.; Xiao, H.; Tian, S.; Huang, Y. A comprehensive review on thermal runaway model of a lithium-ion battery: Mechanism, thermal, mechanical, propagation, gas venting and combustion. *Renew. Energy* **2024**, *229*, 120762. [CrossRef]
57. Feng, X.; Ouyang, M.; Liu, X.; Lu, L.; Xia, Y.; He, X. Thermal runaway mechanism of lithium ion battery for electric vehicles: A review. *Energy Storage Mater.* **2018**, *10*, 246–267. [CrossRef]
58. Lai, Y.; Yang, K.; Liu, H.; Zhang, S.; Zhang, M.; Fan, M. Lithium-ion battery safety warning methods review. *Energy Storage Sci. Technol.* **2020**, *9*, 1926–1932. [CrossRef]
59. Feng, X.; Fang, M.; He, X.; Ouyang, M.; Lu, L.; Wang, H.; Zhang, M. Thermal runaway features of large format prismatic lithium ion battery using extended volume accelerating rate calorimetry. *J. Power Sources* **2014**, *255*, 294–301. [CrossRef]
60. Feng, Y.; Zhou, L.; Ma, H.; Wu, Z.; Zhao, Q.; Li, H.; Zhang, K.; Chen, J. Challenges and advances in wide-temperature rechargeable lithium batteries. *Energy Environ. Sci.* **2022**, *15*, 1711–1759. [CrossRef]
61. Ouyang, D.; Weng, J.; Chen, M.; Wang, J. Impact of high-temperature environment on the optimal cycle rate of lithium-ion battery. *J. Energy Storage* **2020**, *28*, 101242. [CrossRef]
62. Jia, Z.; Wang, Z.; Wang, Q.; Li, X.; Sun, F. Research on Thermal Runaway Mechanism and Safety Risk Control Method of Power Battery in New-Energy Vehicles. *Automot. Eng.* **2022**, *44*, 1689–1705. [CrossRef]
63. Zeng, Y.; Wu, K.; Wang, D.; Wang, Z.; Chen, L. Overcharge investigation of lithium-ion polymer batteries. *J. Power Sources* **2006**, *160*, 1302–1307. [CrossRef]
64. Zhang, L.; Ma, Y.; Cheng, X.; Du, C.; Guan, T.; Cui, Y.; Sun, S.; Zuo, P.; Gao, Y.; Yin, G. Capacity fading mechanism during long-term cycling of over-discharged LiCoO₂/mesocarbon microbeads battery. *J. Power Sources* **2015**, *293*, 1006–1015. [CrossRef]
65. Saito, Y.; Takano, K.; Negishi, A. Thermal behaviors of lithium-ion cells during overcharge. *J. Power Sources* **2001**, *97–98*, 693–696. [CrossRef]
66. Zhu, J.; Wierzbicki, T.; Li, W. A review of safety-focused mechanical modeling of commercial lithium-ion batteries. *J. Power Sources* **2018**, *378*, 153–168. [CrossRef]
67. Chen, Y.; Kang, Y.; Zhao, Y.; Wang, L.; Liu, J.; Li, Y.; Liang, Z.; He, X.; Li, X.; Tavajohi, N.; et al. A review of lithium-ion battery safety concerns: The issues, strategies, and testing standards. *J. Energy Chem.* **2021**, *59*, 83–99. [CrossRef]
68. Chen, S.; Bai, Y. Research progress on thermal runaway mechanism and thermal management technology of lithium-ion power battery. *Bull. Natl. Natl. Sci. Found.* **2023**, *37*, 187–198. [CrossRef]
69. Wang, H.B.; Li, Y.; Wang, Q.Z.; Du, Z.M.; Feng, X.N. Experimental study on the thermal runaway and its propagation of a lithium-ion traction battery with NCM cathode under thermal abuse. *Chin. J. Eng.* **2021**, *43*, 663–675. [CrossRef]

70. Keyser, M.; Pesaran, A.; Li, Q.; Santhanagopalan, S.; Smith, K.; Wood, E.; Ahmed, S.; Bloom, I.; Dufek, E.; Shirk, M.; et al. Enabling fast charging—Battery thermal considerations. *J. Power Sources* **2017**, *367*, 228–236. [CrossRef]
71. Shan, H.; Cao, H.; Xu, X.; Xiao, T.; Hou, G.; Cao, H.; Tang, Y.; Zheng, G. Investigation of self-discharge properties and a new concept of open-circuit voltage drop rate in lithium-ion batteries. *J. Solid State Electrochem.* **2021**, *26*, 163–170. [CrossRef]
72. Vidal, C.; Gross, O.; Gu, R.; Kollmeyer, P.; Emadi, A. xEV Li-ion battery low-temperature effects. *IEEE Trans. Veh. Technol.* **2019**, *68*, 4560–4572. [CrossRef]
73. Luo, H.; Wang, Y.; Feng, Y.-H.; Fan, X.-Y.; Han, X.; Wang, P.-F. Lithium-ion batteries under low-temperature environment: Challenges and prospects. *Materials* **2022**, *15*, 8166. [CrossRef] [PubMed]
74. Liu, Y.; Fu, H.; Gao, C.; Wen, J.; Guo, R.; Luo, W.; Zhou, J.; Lu, B. Solvation Structure Dual-Regulator Enabled Multidimensional Improvement for Low-Temperature Potassium Ion Batteries. *Adv. Energy Mater.* **2024**, *2403562*. [CrossRef]
75. Yi, X.; Fu, H.; Rao, A.M.; Zhang, Y.; Zhou, J.; Wang, C.; Lu, B. Safe electrolyte for long-cycling alkali-ion batteries. *Nat. Sustain.* **2024**, *7*, 326–337. [CrossRef]
76. Piao, N.; Gao, X.; Yang, H.; Guo, Z.; Hu, G.; Cheng, H.-M.; Li, F. Challenges and development of lithium-ion batteries for low temperature environments. *eTransportation* **2022**, *11*, 100145. [CrossRef]
77. Badami, P.; Opitz, A.; Shen, L.; Vaidya, R.; Mayyas, A.; Knoop, K.; Razdan, A.; Kannan, A. Performance of 26650 Li-ion cells at elevated temperature under simulated PHEV drive cycles. *Int. J. Hydrol. Energy* **2017**, *42*, 12396–12404. [CrossRef]
78. Ouyang, D.; Weng, J.; Hu, J.; Liu, J.; Chen, M.; Huang, Q.; Wang, J. Effect of high temperature circumstance on lithium-ion battery and the application of phase change material. *J. Electrochem. Soc.* **2019**, *166*, A559–A567. [CrossRef]
79. Zhang, G.; Wei, X.; Chen, S.; Wei, G.; Zhu, J.; Wang, X.; Han, G.; Dai, H. Research on the impact of high-temperature aging on the thermal safety of lithium-ion batteries. *J. Energy Chem.* **2023**, *87*, 378–389. [CrossRef]
80. Ping, P.; Peng, R.; Kong, D.; Chen, G.; Wen, J. Investigation on thermal management performance of PCM-fin structure for Li-ion battery module in high-temperature environment. *Energy Convers. Manag.* **2018**, *176*, 131–146. [CrossRef]
81. Xiong, R.; Pan, Y.; Shen, W.; Li, H.; Sun, F. Lithium-ion battery aging mechanisms and diagnosis method for automotive applications: Recent advances and perspectives. *Renew. Sustain. Energy Rev.* **2020**, *131*, 110048. [CrossRef]
82. Zhang, Z.; Li, M. Research on the temperature rise characteristics of lithium-ion power battery. *Automot. Eng.* **2010**, *32*, 320–323. [CrossRef]
83. Zhu, C.; Lu, J.; Li, X.; Su, W. Thermal modelling of square lithium-ion battery packs. *Automot. Eng.* **2012**, *34*, 339–344+350. [CrossRef]
84. Sun, B.; Li, M.; Zhang, W.; Wang, J.; Zhang, Y. Quantitative study of temperature inconsistency on the discharge performance of series-connected battery packs. *Power Syst. Prot. Control* **2023**, *51*, 150–158. [CrossRef]
85. Wei, Z.; Yuan, W.; Li, Z. Study on the influence of heat transfer mechanism on thermal runaway spreading of lithium-ion battery packs. *Ind. Saf. Environ. Prot.* **2021**, *47*, 1–5.
86. Peng, Y.; Wang, H.; Jin, C.; Huang, W.; Zhang, F.; Li, B.; Ju, W.; Xu, C.; Feng, X.; Ouyang, M. Thermal runaway induced gas hazard for cell-to-pack (CTP) lithium-ion battery pack. *J. Energy Storage* **2023**, *72*, 108324. [CrossRef]
87. Ye, Z.; Fu, X. Experimental and simulation investigation on suppressing thermal runaway in battery pack. *Sci. Rep.* **2024**, *14*, 12723. [CrossRef]
88. Fu, H.; Wang, J.; Li, L.; Gong, J.; Wang, X. Numerical study of mini-channel liquid cooling for suppressing thermal runaway propagation in a lithium-ion battery pack. *Appl. Therm. Eng.* **2023**, *234*, 121349. [CrossRef]
89. Broatch, A.; Olmeda, P.; Margot, X.; Agizza, L. A generalized methodology for lithium-ion cells characterization and lumped electro-thermal modelling. *Appl. Therm. Eng.* **2022**, *217*, 119174. [CrossRef]
90. Hu, X.; Liu, W.; Lin, X.; Xie, Y. A comparative study of control-oriented thermal models for cylindrical Li-ion batteries. *IEEE Trans. Transp. Electrif.* **2019**, *5*, 1237–1253. [CrossRef]
91. Xie, Y.; Li, W.; Hu, X.; Zou, C.; Feng, F.; Tang, X. Novel mesoscale electrothermal modeling for lithium-ion batteries. *IEEE Trans. Power Electron.* **2019**, *35*, 2595–2614. [CrossRef]
92. Mevawalla, A.; Panchal, S.; Tran, M.-K.; Fowler, M.; Fraser, R. One dimensional fast computational partial differential model for heat transfer in lithium-ion batteries. *J. Energy Storage* **2021**, *37*, 102471. [CrossRef]
93. Ahn, Y.J. Finite Element Analysis of the Mechanical Response for Cylindrical Lithium-Ion Batteries with the Double-Layer Windings. *Energies* **2024**, *17*, 3357. [CrossRef]
94. He, C.; Liu, Y.; Huang, X.; Wan, S.; Chen, Q.; Sun, J.; Zhao, T. A transient multi-path decentralized resistance-capacity network model for prismatic lithium-ion batteries based on genetic algorithm optimization. *Energy Convers. Manag.* **2023**, *300*, 117894. [CrossRef]
95. Samanta, A.; Williamson, S.S. A comprehensive review of lithium-ion cell temperature estimation techniques applicable to health-conscious fast charging and smart battery management systems. *Energies* **2021**, *14*, 5960. [CrossRef]
96. Tang, Y.; Wu, L.; Wei, W.; Wen, D.; Guo, Q.; Liang, W.; Xiao, L. Study of the thermal properties during the cyclic process of lithium ion power batteries using the electrochemical-thermal coupling model. *Appl. Therm. Eng.* **2018**, *137*, 11–22. [CrossRef]
97. Guo, M.; Sikha, G.; White, R.E. Single-particle model for a lithium-ion cell: Thermal behavior. *J. Electrochem. Soc.* **2011**, *158*, A122–A132. [CrossRef]
98. Kang, D.; Lee, P.-Y.; Yoo, K.; Kim, J. Internal thermal network model-based inner temperature distribution of high-power lithium-ion battery packs with different shapes for thermal management. *J. Energy Storage* **2019**, *27*, 101017. [CrossRef]

99. Kim, Y.; Mohan, S.; Siegel, J.B.; Stefanopoulou, A.G.; Ding, Y. The estimation of temperature distribution in cylindrical battery cells under unknown cooling conditions. *IEEE Trans. Control Syst. Technol.* **2014**, *22*, 2277–2286. [[CrossRef](#)]
100. Al-Hallaj, S.; Selman, J. Thermal modeling of secondary lithium batteries for electric vehicle/hybrid electric vehicle applications. *J. Power Sources* **2002**, *110*, 341–348. [[CrossRef](#)]
101. Forgez, C.; Do, D.V.; Friedrich, G.; Morcrette, M.; Delacourt, C. Thermal modeling of a cylindrical LiFePO₄/graphite lithium-ion battery. *J. Power Sources* **2009**, *195*, 2961–2968. [[CrossRef](#)]
102. Du, S.; Lai, Y.; Ai, L.; Ai, L.; Cheng, Y.; Tang, Y.; Jia, M. An investigation of irreversible heat generation in lithium ion batteries based on a thermo-electrochemical coupling method. *Appl. Therm. Eng.* **2017**, *121*, 501–510. [[CrossRef](#)]
103. Mei, W.; Chen, H.; Sun, J.; Wang, Q. Numerical study on tab dimension optimization of lithium-ion battery from the thermal safety perspective. *Appl. Therm. Eng.* **2018**, *142*, 148–165. [[CrossRef](#)]
104. Huang, Y.; Lai, X.; Ren, D.; Kong, X.; Han, X.; Lu, L.; Zheng, Y. Thermal and stoichiometry inhomogeneity investigation of large-format lithium-ion batteries via a three-dimensional electrochemical-thermal coupling model. *Electrochim. Acta* **2023**, *468*, 143212. [[CrossRef](#)]
105. Tourani, A.; White, P.; Ivey, P. A multi scale multi-dimensional thermo electrochemical modelling of high capacity lithium-ion cells. *J. Power Sources* **2014**, *255*, 360–367. [[CrossRef](#)]
106. Song, L.; Evans, J.W. Electrochemical-thermal model of lithium polymer batteries. *J. Electrochem. Soc.* **2000**, *147*, 2086–2095. [[CrossRef](#)]
107. Ludwig, S.; Steinhardt, M.; Jossen, A. Determination of internal temperature differences for various cylindrical lithium-ion batteries using a pulse resistance approach. *Batteries* **2022**, *8*, 60. [[CrossRef](#)]
108. Wu, M.-S.; Liu, K.; Wang, Y.-Y.; Wan, C.-C. Heat dissipation design for lithium-ion batteries. *J. Power Sources* **2002**, *109*, 160–166. [[CrossRef](#)]
109. Li, D.; Yang, K.; Chen, S.; Wu, F. Thermal behavior of overcharged nickel/metal hydride batteries. *J. Power Sources* **2008**, *184*, 622–626. [[CrossRef](#)]
110. Chen, S.; Wan, C.; Wang, Y. Thermal analysis of lithium-ion batteries. *J. Power Sources* **2004**, *140*, 111–124. [[CrossRef](#)]
111. Xu, M.; Zhang, Z.; Wang, X.; Jia, L.; Yang, L. A pseudo three-dimensional electrochemical-thermal model of a prismatic LiFePO₄ battery during discharge process. *Energy* **2015**, *80*, 303–317. [[CrossRef](#)]
112. Huo, W.; He, H.; Sun, F. Electrochemical-thermal modeling for a ternary lithium ion battery during discharging and driving cycle testing. *RSC Adv.* **2015**, *5*, 57599–57607. [[CrossRef](#)]
113. Liu, X.; Li, Y.; Kang, Y.; Zhao, G.; Duan, B.; Zhang, C. An accurate co-estimation of core temperature and state of charge for Lithium-ion batteries with electro-thermal model. *IEEE J. Emerg. Sel. Top. Power Electron.* **2023**, *12*, 231–241. [[CrossRef](#)]
114. Lin, X.; Perez, H.E.; Siegel, J.B.; Stefanopoulou, A.G.; Li, Y.; Anderson, R.D.; Ding, Y.; Castanier, M.P. Online parameterization of lumped thermal dynamics in cylindrical lithium-ion batteries for core temperature estimation and health monitoring. *IEEE Trans. Control Syst. Technol.* **2012**, *21*, 1745–1755. [[CrossRef](#)]
115. Lin, X.; Perez, H.E.; Mohan, S.; Siegel, J.B.; Stefanopoulou, A.G.; Ding, Y.; Castanier, M.P. A lumped-parameter electro-thermal model for cylindrical batteries. *J. Power Sources* **2014**, *257*, 1–11. [[CrossRef](#)]
116. Chen, L.; Hu, M.; Cao, K.; Li, S.; Su, Z.; Jin, G.; Fu, C. Core temperature estimation based on electro-thermal model of lithium-ion batteries. *Int. J. Energy Res.* **2020**, *44*, 5320–5333. [[CrossRef](#)]
117. Zhang, C.; Li, K.; Deng, J. Real-time estimation of battery internal temperature based on a simplified thermoelectric model. *J. Power Sources* **2016**, *302*, 146–154. [[CrossRef](#)]
118. Catalano, A.P.; Scognamillo, C.; Piccirillo, F.; Iasiello, M.; Guerriero, P.; Bianco, N.; Codecasa, L.; D'alessandro, V. Thermo-Electrochemical FEM and Circuit Simulations of Li-Ion Batteries. *IEEE Trans. Compon. Packag. Manuf. Technol.* **2023**, *13*, 1088–1095. [[CrossRef](#)]
119. Pang, H.; Guo, L.; Wu, L.; Jin, J.; Zhang, F.; Liu, K. A novel extended Kalman filter-based battery internal and surface temperature estimation based on an improved electro-thermal model. *J. Energy Storage* **2021**, *41*, 102854. [[CrossRef](#)]
120. Kumar, P.; Balasingam, B.; Rankin, G.; Pattipati, K.R. Battery thermal model identification and surface temperature prediction. In Proceedings of the IECON 2021—47th Annual Conference of the IEEE Industrial Electronics Society, Toronto, ON, Canada, 13–16 October 2021. [[CrossRef](#)]
121. Mahboubi, D.; Gavzani, I.J.; Saidi, M.H.; Ahmadi, N. Developing an electro-thermal model to determine heat generation and thermal properties in a lithium-ion battery. *J. Therm. Anal. Calorim.* **2022**, *147*, 12253–12267. [[CrossRef](#)]
122. Hu, Y.; Yurkovich, S.; Guezennec, Y.; Yurkovich, B. Electro-thermal battery model identification for automotive applications. *J. Power Sources* **2010**, *196*, 449–457. [[CrossRef](#)]
123. Wang, C.; Li, C.; Wang, G.; Zhang, C.; Cui, N. Fast identification method for thermal model parameters of Lithium-ion battery based on discharge temperature rise. *J. Energy Storage* **2021**, *44*, 103362. [[CrossRef](#)]
124. Sun, L.; Sun, W.; You, F. Core temperature modelling and monitoring of lithium-ion battery in the presence of sensor bias. *Appl. Energy* **2020**, *271*, 115243. [[CrossRef](#)]
125. Dey, S.; Biron, Z.A.; Tatipamula, S.; Das, N.; Mohon, S.; Ayalew, B.; Pisú, P. Model-based real-time thermal fault diagnosis of Lithium-ion batteries. *Control Eng. Pract.* **2016**, *56*, 37–48. [[CrossRef](#)]
126. Lin, X.; Perez, H.E.; Siegel, J.B.; Stefanopoulou, A.G. Robust estimation of battery system temperature distribution under sparse sensing and uncertainty. *IEEE Trans. Control Syst. Technol.* **2019**, *28*, 753–765. [[CrossRef](#)]

127. Srinivasan, R.; Carkhuff, B.G.; Butler, M.H.; Baisden, A.C. Instantaneous measurement of the internal temperature in lithium-ion rechargeable cells. *Electrochim. Acta* **2011**, *56*, 6198–6204. [[CrossRef](#)]
128. Schmidt, J.P.; Arnold, S.; Loges, A.; Werner, D.; Wetzel, T.; Ivers-Tiffée, E. Measurement of the internal cell temperature via impedance: Evaluation and application of a new method. *J. Power Sources* **2013**, *243*, 110–117. [[CrossRef](#)]
129. Richardson, R.R.; Howey, D.A. Sensorless battery internal temperature estimation using a Kalman filter with impedance measurement. *IEEE Trans. Sustain. Energy* **2015**, *6*, 1190–1199. [[CrossRef](#)]
130. Spinner, N.S.; Love, C.T.; Rose-Pehrsson, S.L.; Tuttle, S.G. Expanding the operational limits of the single-point impedance diagnostic for internal temperature monitoring of lithium-ion batteries. *Electrochim. Acta* **2015**, *174*, 488–493. [[CrossRef](#)]
131. Rajmakers, L.; Danilov, D.; van Lammeren, J.; Lammers, M.; Notten, P. Sensorless battery temperature measurements based on electrochemical impedance spectroscopy. *J. Power Sources* **2014**, *247*, 539–544. [[CrossRef](#)]
132. Xiang, D.; Yang, C.; Li, H.; Zhou, Y.; Zhu, S.; Li, Y. Online monitoring of lithium-ion battery internal temperature using PWM switching oscillations. *IEEE Trans. Power Electron.* **2022**, *38*, 1166–1177. [[CrossRef](#)]
133. Rajmakers, L.H.J.; Danilov, D.L.; van Lammeren, J.P.M.; Lammers, T.J.G.; Bergveld, H.J.; Notten, P.H.L. Non-zero intercept frequency: An accurate method to determine the integral temperature of li-ion batteries. *IEEE Trans. Ind. Electron.* **2016**, *63*, 3168–3178. [[CrossRef](#)]
134. Hussein, A.A.; Fardoun, A.A. An adaptive sensorless measurement technique for internal temperature of Li-ion batteries using impedance phase spectroscopy. *IEEE Trans. Ind. Appl.* **2020**, *56*, 3043–3051. [[CrossRef](#)]
135. Moral, C.G.; Laborda, D.F.; Alonso, L.S.; Guerrero, J.M.; Fernandez, D.; Pereda, C.R.; Reigosa, D.D. Battery internal resistance estimation using a battery balancing system based on switched capacitors. *IEEE Trans. Ind. Appl.* **2020**, *56*, 5363–5374. [[CrossRef](#)]
136. Jiang, Y.; Yu, Y.; Huang, J.; Cai, W.; Marco, J. Li-ion battery temperature estimation based on recurrent neural networks. *Sci. China Technol. Sci.* **2021**, *64*, 1335–1344. [[CrossRef](#)]
137. Naguib, M.; Kollmeyer, P.; Vidal, C.; Emadi, A. Accurate surface temperature estimation of lithium-ion batteries using feedforward and recurrent artificial neural networks. In Proceedings of the 2021 IEEE Transportation Electrification Conference & Expo (ITEC), Chicago, IL, USA, 21–25 June 2021. [[CrossRef](#)]
138. Ojo, O.; Lang, H.; Kim, Y.; Hu, X.; Mu, B.; Lin, X. A neural network based method for thermal fault detection in lithium-ion batteries. *IEEE Trans. Ind. Electron.* **2020**, *68*, 4068–4078. [[CrossRef](#)]
139. Jiang, L.; Yan, C.; Zhang, X.; Zhou, B.; Cheng, T.; Zhao, J.; Gu, J. Temperature prediction of battery energy storage plant based on EGA-BiLSTM. *Energy Rep.* **2022**, *8*, 1009–1018. [[CrossRef](#)]
140. Yao, Q.; Lu, D.D.-C.; Lei, G. A surface temperature estimation method for lithium-ion battery using enhanced GRU-RNN. *IEEE Trans. Transp. Electrif.* **2022**, *9*, 1103–1112. [[CrossRef](#)]
141. Liu, K.; Li, K.; Peng, Q.; Guo, Y.; Zhang, L. Data-Driven Hybrid Internal Temperature Estimation Approach for Battery Thermal Management. *Complexity* **2018**, *2018*, 9642892. [[CrossRef](#)]
142. Liu, Y.; Huang, Z.; Wu, Y.; Yan, L.; Jiang, F.; Peng, J. An online hybrid estimation method for core temperature of Lithium-ion battery with model noise compensation. *Appl. Energy* **2022**, *327*, 120037. [[CrossRef](#)]
143. Surya, S.; Samanta, A.; Marcis, V.; Williamson, S. Hybrid electrical circuit model and deep learning-based core temperature estimation of lithium-ion battery cell. *IEEE Trans. Transp. Electrif.* **2022**, *8*, 3816–3824. [[CrossRef](#)]
144. Feng, F.; Teng, S.; Liu, K.; Xie, J.; Xie, Y.; Liu, B.; Li, K. Co-estimation of lithium-ion battery state of charge and state of temperature based on a hybrid electrochemical-thermal-neural-network model. *J. Power Sources* **2020**, *455*, 227935. [[CrossRef](#)]
145. Vaidya, S.; Depernet, D.; Lagrouche, S.; Chrenko, D. State of temperature detection of Li-ion batteries by intelligent gray box model. *J. Power Sources* **2023**, *585*, 233624. [[CrossRef](#)]
146. Cho, G.; Wang, M.; Kim, Y.; Kwon, J.; Su, W. A physics-informed machine learning approach for estimating lithium-ion battery temperature. *IEEE Access* **2022**, *10*, 88117–88126. [[CrossRef](#)]
147. Cho, G.; Zhu, D.; Campbell, J.J.; Wang, M. An LSTM-PINN hybrid method to estimate lithium-ion battery pack temperature. *IEEE Access* **2022**, *10*, 100594–100604. [[CrossRef](#)]

Disclaimer/Publisher’s Note: The statements, opinions and data contained in all publications are solely those of the individual author(s) and contributor(s) and not of MDPI and/or the editor(s). MDPI and/or the editor(s) disclaim responsibility for any injury to people or property resulting from any ideas, methods, instructions or products referred to in the content.